

2-28-2017

# Embryonic transcription factor expression in mice predicts medial amygdala neuronal identity and sex-specific responses to innate behavioral cues.

Julieta E Lischinsky

Katie Sokolowski


Li Peijun

Shigeyuki Esumi

Yasmin Kamal

*See next page for additional authors*

Follow this and additional works at: [http://hsrc.himmelfarb.gwu.edu/smhs\\_peds\\_facpubs](http://hsrc.himmelfarb.gwu.edu/smhs_peds_facpubs)

 Part of the [Embryonic Structures Commons](#), [Neurology Commons](#), and the [Pediatrics Commons](#)

---

## APA Citation

Lischinsky, J., Sokolowski, K., Peijun, L., Esumi, S., Kamal, Y., Goodrich, M., Oboti, L., Hammond, T., Krishnamoorthy, M., Feldman, D., Huntsman, M., Liu, J., & Corbin, J. (2017). Embryonic transcription factor expression in mice predicts medial amygdala neuronal identity and sex-specific responses to innate behavioral cues.. *Elife*, 6 (). <http://dx.doi.org/10.7554/eLife.21012>

This Journal Article is brought to you for free and open access by the Pediatrics at Health Sciences Research Commons. It has been accepted for inclusion in Pediatrics Faculty Publications by an authorized administrator of Health Sciences Research Commons. For more information, please contact [hsrc@gwu.edu](mailto:hsrc@gwu.edu).

---

**Authors**

Julieta E Lischinsky, Katie Sokolowski, Li Peijun, Shigeyuki Esumi, Yasmin Kamal, Meredith Goodrich, Livio Oboti, Timothy R Hammond, Meera Krishnamoorthy, Daniel Feldman, Molly Huntsman, Judy Liu, and Joshua G Corbin

1 **Embryonic transcription factor expression in mice predicts medial amygdala neuronal**  
2 **identity and sex-specific responses to innate behavioral cues.**

3

4 Lischinsky J.E.<sup>1,2</sup>, Sokolowski K.<sup>2</sup>, Li, P.<sup>2</sup>, Esumi S.<sup>2,3</sup>, Kamal Y.<sup>2</sup>, Goodrich M.<sup>2</sup>, Oboti L.<sup>2</sup>,  
5 Hammond T.R.<sup>2</sup>, Krishnamoorthy, M.<sup>2</sup>, Feldman D.<sup>2</sup>, Huntsman M.M.<sup>4</sup>, Liu J.<sup>2</sup> & Corbin J.G.<sup>2</sup>

6

7 <sup>1</sup>Institute for Biomedical Sciences, The George Washington University, Washington DC;

8 <sup>2</sup>Center for Neuroscience Research, Children's National Medical Center, Washington, DC;

9 <sup>3</sup>Graduate School of Medical Sciences, Kumamoto-University, Kumamoto City, Japan;

10 <sup>4</sup>Department of Pediatrics, University of Colorado School of Medicine, Aurora, Colorado.

11

12 **Abstract**

13 The medial subnucleus of the amygdala (MeA) plays a central role in processing sensory cues  
14 required for innate behaviors. However, whether there is a link between developmental programs  
15 and the emergence of inborn behaviors remains unknown. Our previous studies revealed that the  
16 telencephalic preoptic area (POA) embryonic niche is a novel source of MeA destined  
17 progenitors. Here, we show that the POA is comprised of distinct progenitor pools  
18 complementarily marked by the transcription factors *Dbx1* and *Foxp2*. As determined by  
19 molecular and electrophysiological criteria this embryonic parcellation predicts postnatal MeA  
20 inhibitory neuronal subtype identity. We further find that *Dbx1*-derived and *Foxp2*<sup>+</sup> cells in the  
21 MeA are differentially activated in response to innate behavioral cues in a sex-specific manner.  
22 Thus, developmental transcription factor expression is predictive of MeA neuronal identity and  
23 sex-specific neuronal responses, providing a potential developmental logic for how innate  
24 behaviors could be processed by different MeA neuronal subtypes.

25

26 Word count: 150

27

28

29

30

31

32

33

34

## 35 **Introduction**

36 One of the major functions of the limbic system is to integrate conspecific and non-conspecific  
37 environmental cues with social and survival salience to generate appropriate behavioral  
38 responses (Sokolowski, Corbin 2012, Stowers, Cameron & Keller 2013). The medial subnucleus  
39 of the amygdala (MeA) serves as a hub in this function, residing only two synapses away from  
40 sensory neurons in the olfactory bulb (Dulac, Wagner 2006, Sokolowski, Corbin 2012). The  
41 MeA along with bed nucleus of the stria terminalis (BNST) and multiple nuclei of the  
42 hypothalamus including the ventromedial hypothalamus, form a core limbic circuit largely  
43 dedicated to processing innate behaviors (Dulac, Wagner 2006, Gross, Canteras 2012, Choi et al.  
44 2005). Classical studies investigating patterns of neuronal activation in response to behavioral or  
45 olfactory cues (Kollack, Newman 1992, Erskine 1993), lesioning studies and more recent  
46 optogenetic approaches (Vochteloo, Koolhaas 1987, Takahashi, Gladstone 1988, Kondo 1992,  
47 Hong, Kim & Anderson 2014) have revealed a central role for the MeA in the regulation of  
48 innate behaviors such as aggression, mating and predator avoidance.

49 In addition to the processing of innate cues, the MeA is one of many known sexually  
50 dimorphic regions of the brain, with differences in numbers of neurons, glia, and synaptic  
51 organization between males and females (Cooke, Woolley 2005, Johnson, Breedlove & Jordan  
52 2008, McCarthy, Arnold 2011). The critical role that the MeA plays in regulating sex-specific  
53 behaviors is reflected in the high expression levels of steroid hormone pathway proteins such as  
54 aromatase, estrogen receptor and androgen receptor (Wu et al. 2009, Juntti et al. 2010, Unger et  
55 al. 2015). MeA neuronal subpopulations expressing different combinations of these proteins  
56 have been shown to regulate aggression or mating behaviors in male and female mice (Juntti et

57 al. 2010, Hong, Kim & Anderson 2014, Unger et al. 2015). Nonetheless, understanding how  
58 developmental programs are linked to behavioral processing in the MeA remains unknown.

59 As unlearned behaviors are largely inborn, we reasoned that there must be embryonic  
60 developmental programs that guide formation of sub-circuitry dedicated for different innate  
61 behaviors. Previous studies of MeA development revealed that progenitors located at the  
62 telencephalic-diencephalic border are a major source of MeA neuronal populations (Zhao et al.  
63 2008, Hirata et al. 2009, Soma et al. 2009, Garcia-Moreno et al. 2010). Our previous work  
64 revealed that one of these progenitor populations is defined by the transient expression of the  
65 developmentally regulated transcription factor, *Dbx1*, which in turn generate a subclass of MeA  
66 putative inhibitory projection neurons (Hirata et al. 2009). However, the MeA is also comprised  
67 of diverse populations of local interneurons and both excitatory and inhibitory output neurons  
68 (Bian 2013, Keshavarzi et al. 2014). This suggests the contribution of other progenitor  
69 subpopulations, perhaps also originating from the POA to MeA neuronal diversity, populations  
70 which may in turn play different roles in innate behavioral processing.

71 Here, we demonstrate that in addition to *Dbx1* expression, a subset of MeA embryonic  
72 progenitors are complementarily marked by expression of *Foxp2*, a forkhead transcription factor  
73 implicated in the development and function of neurons and required in the motor coordinating  
74 centers of the brain for the appropriate production of speech (French, Fisher 2014). We find this  
75 embryonic parcellation interestingly persists into postnatal stages where *Dbx1*-derived and  
76 *Foxp2*<sup>+</sup> MeA neurons are separate, non-overlapping inhibitory output neuronal subpopulations.  
77 Strikingly, both subpopulations are activated during specific innate behaviors in a sex-specific  
78 manner. Thus, our findings link developmental patterning to innate behavioral processing and  
79 further provide an embryonic developmental framework for how these behaviors may emerge.

## 80 Results

### 81 *Dbx1 and Foxp2 expression segregates embryonic and postnatal MeA subpopulations*

82 Our previous work along with the work of others revealed that the telencephalic-diencephalic  
83 border is a major source of neurons that will populate the MeA (Zhao et al. 2008, Hirata et al.  
84 2009, Soma et al. 2009, Garcia-Moreno et al. 2010). Our previous studies (Hirata et al. 2009)  
85 revealed that the preoptic area (POA), which lies on the telencephalic side of this border (Flames  
86 et al. 2007), is a source of *Dbx1*<sup>+</sup> progenitors fated to generate a subpopulation of MeA  
87 inhibitory output neurons. Our previous studies further revealed that progenitors arising from  
88 ventral telencephalic *Shh*<sup>+</sup> and *Nkx2.1*<sup>+</sup> domains also contributed diverse neuronal  
89 subpopulations to the MeA (Carney et al. 2010). Thus, while a molecular map of MeA  
90 embryonic niche diversity is beginning to emerge, the diversity of mature neurons derived from  
91 this niche and whether there is a link between embryonic identity, mature identity and function  
92 remains unknown. Moreover, as these previously identified subpopulations only generate a  
93 subset of MeA neurons, we reasoned that there must be other transcription factor marked  
94 progenitor populations within the telencephalic-diencephalic niche.

95 Here, in addition to *Dbx1*<sup>+</sup> progenitors, we observed a progenitor population comprised  
96 of *Foxp2*<sup>+</sup> cells, residing primarily in the putative subventricular zone (SVZ) of the POA  
97 (**Figure 1a-f, s**). Interestingly, during embryogenesis, *Dbx1*-derived and *Foxp2*<sup>+</sup> progenitor  
98 populations were non-overlapping (**Figure 1a-l**). Both populations were also generally distinct  
99 from *OTP*<sup>+</sup> progenitors (**Figure 1-Figure Supplement 1a-i**), a population previously shown to  
100 define a subset of MeA-fated progenitors (Garcia-Moreno et al. 2010). We next investigated  
101 whether *Foxp2*<sup>+</sup> progenitors overlapped with ventral telencephalic populations derived from *Shh*  
102 or *Nkx6.2* lineages, which also encompass the POA (Carney et al., 2010; Fogarty et al., 2007).

103 We found embryonic Foxp2+ cells were not derived from either lineage (~5% overlap) (**Figure**  
104 **1- Figure supplement 2**) further expanding our knowledge of the molecular diversity of the  
105 MeA niche.

106 Interestingly, this embryonic molecular parcellation persisted into adulthood as *Dbx1*-  
107 derived and Foxp2+ cells remained non-overlapping across the rostro-caudal extent of the  
108 postnatal MeA (**Figure 1m-r; Figure 1-Figure supplement 3**). Similarly, postnatally, the *Dbx1*-  
109 derived and Foxp2+ neurons remained distinct from OTP+ cells (**Figure 1-Figure supplement**  
110 **1j-x**). Taken together, these findings reveal that *Dbx1*-derived and Foxp2+ populations, although  
111 appearing to derive from the same embryonic niche, remain distinct subpopulations from  
112 embryonic development to adulthood (**Figure 1t**), a novel finding that we hypothesized has  
113 implications for later subtype identity and function, explored in the next sets of experiments.

114

#### 115 *Foxp2+ neurons in the postnatal amygdala are inhibitory*

116 Our previous work revealed that MeA *Dbx1*-derived neurons are a subclass of inhibitory  
117 neurons, likely projection as opposed to local interneurons (Hirata et al. 2009). However, the  
118 identity of MeA Foxp2+ neurons remains unknown. Therefore, we next examined whether adult  
119 MeA Foxp2+ cells were neurons or glia. Our analysis revealed that 81%±2.6 of Foxp2+ cells  
120 expressed NeuN, a pan neuronal marker (Mullen, Buck & Smith 1992) (**Figure 2a-d**), with none  
121 co-expressing the oligodendrocyte marker, CC1 (Koenning et al. 2012) (**Figure 2e-h**). We next  
122 wanted to determine if Foxp2+ neurons were excitatory or inhibitory. We found that only  
123 3%±1.2 of Foxp2+ cells were derived from the *Emx1*-lineage, a broad marker of excitatory  
124 neurons (Gorski et al. 2002) (**Figure 2i-l**). We further found that 22%±6.6 of Foxp2+ cells  
125 expressed the inhibitory marker Calbindin (**Figure 2m-p**), with a smaller percentage of Foxp2+



126 cells ( $15\% \pm 2.5$ ) expressing nNOS (**Figure 2q-t**), or somatostatin ( $5\% \pm 0.6$ ) (**Figure 2u-x**),  
127 inhibitory markers that mark a subset of MeA output neurons (Tanaka et al. 1997) and  
128 interneurons (Petilla Interneuron Nomenclature Group et al. 2008), respectively. Collectively,  
129 although we did not fully assess all putative inhibitory markers, these data reveal that  $Foxp2+$   
130 MeA are not excitatory and are likely inhibitory (**Figure 2y**).

131 As neither *Dbx1*-derived nor  $Foxp2+$  cells expressed  $OTP+$ , we therefore investigated the  
132 identity of this population. We found that  $1\% \pm 0.4$  of  $OTP+$  cells were derived from the *Emx1*-  
133 lineage, and  $13.5\% \pm 9.1$  co-expressed *CAMKII $\alpha$*  (Jones, Huntley & Benson 1994), both  
134 excitatory markers. In contrast, we observed  $56\% \pm 18.9$  of  $OTP+$  cells co-expressed calbindin,  
135 while none ( $0\% \pm 0.1$ ) co-expressed somatostatin (**Figure 2- Figure supplement 1**). Therefore,  
136 similar to *Dbx1*-derived and  $Foxp2+$  neurons, the majority of  $OTP+$  cells appear to be inhibitory.

137

### 138 *Dbx1*-derived and *Foxp2+* neurons possess distinct electrophysiological properties

139 To determine if *Dbx1*-derived and the  $Foxp2+$  populations are functionally distinct subclasses,  
140 we next examined their electrophysiological properties. Previous studies (Bian 2013, Keshavarzi  
141 et al. 2014) revealed a significant diversity in intrinsic electrophysiological properties of MeA  
142 local and projection neurons. Here, we found that the majority (19/28) of *Dbx1*-derived neurons  
143 were characterized by a regular, tonic spiking pattern with 3-4 spikes at rheobase (**Figure 3a**). In  
144 contrast, the majority (15/23) of  $Foxp2+$  neurons were distinguished by a phasic firing pattern  
145 and displayed a single or double spike upon repolarization after hyperpolarization, a profile  
146 characteristic of inhibitory neurons (Llinas 1988) (**Figure 3b**). *Dbx1*-derived and *Foxp2*-derived  
147 neurons (confirmed  $Foxp2+$  by immunohistochemistry) also displayed significant differences in  
148 resting membrane potential, input resistance, capacitance, and action potential frequency but not

149 in rheobase (**Figure 3c-g**). In addition, the presence of spines in Foxp2+ neurons (**Figure 3-**  
150 **Figure supplement 1**) suggested that similar to *Dbx1*-derived neurons, Foxp2+ neurons are  
151 projection neurons. This reveals that despite both populations being inhibitory, the *Dbx1*-derived  
152 and the Foxp2+ populations possess distinct firing patterns.

153 We further analyzed spontaneous excitatory post-synaptic currents (sEPSCs), a measure  
154 of excitatory inputs. *Dbx1*-derived neurons received significantly more frequent and greater  
155 amplitude of EPSCs than Foxp2+ neurons (**Figure 3h-l**). This suggests that *Dbx1*-derived MeA  
156 neurons receive a greater number and/or stronger excitatory inputs than Foxp2+ neurons. In  
157 summary, a combination of neuronal marker expression (**Figure 2**) and electrophysiological  
158 (**Figure 3**) analyses, combined with our previous analysis (Hirata et al. 2009) revealed that  
159 *Dbx1*-derived and Foxp2+ neurons are distinct subclasses of inhibitory, and likely projection  
160 neurons.

161

### 162 *Molecular identity of Dbx1-derived and Foxp2+ postnatal MeA cells*

163 Based on the above analyses revealing that *Dbx1*-derived and Foxp2+ neurons are separate  
164 subclasses, we next wanted to determine whether these two populations express different  
165 combinations of steroid pathway proteins previously associated with MeA function such as  
166 estrogen receptor-alpha (ER $\alpha$ ), aromatase and androgen receptor (AR) (Wu et al. 2009, Juntti et  
167 al. 2010, Unger et al. 2015). As the MeA is a sexually dimorphic nucleus (Cooke, Woolley 2005,  
168 McCarthy, Arnold 2011, Johnson, Breedlove & Jordan 2008), we characterized the expression of  
169 these markers in both male and female mice (**Figure 4, Figure 4-Figure supplement 1, Figure**  
170 **4-Figure supplement 2**). We found that *Dbx1*-derived and Foxp2+ cells in males expressed  
171 ER $\alpha$  to the same extent (28.4% $\pm$ 4.8 in *Dbx1*-derived cells; 24.0% $\pm$ 7.2 in Foxp2+ cells).

172 However, *Dbx1*-derived and Foxp2<sup>+</sup> cells in females showed significant differences in ER $\alpha$   
173 expression (45% $\pm$ 3.4 in *Dbx1*-derived cells; 24.8% $\pm$ 5.8 in Foxp2<sup>+</sup> cells) (**Figure 4a-g**). The  
174 majority of *Dbx1*-derived cells expressed aromatase both in males (61.7% $\pm$ 7.6) and females  
175 (52.4% $\pm$ 5.2), which was at a significantly higher level than in Foxp2<sup>+</sup> cells in males (0.12% $\pm$ 0)  
176 and females (7.2% $\pm$ 6.0) (**Figure 4h-n**). There were no subpopulation differences in AR  
177 expression as both *Dbx1*-derived and Foxp2<sup>+</sup> neurons in both males (26.8% $\pm$ 4.1 in *Dbx1*-  
178 derived cells; 16.2% $\pm$ 3.2 in Foxp2<sup>+</sup> cells) and females (8.4% $\pm$ 3.6 in *Dbx1*-derived cells;  
179 7.0% $\pm$ 1.8 in Foxp2<sup>+</sup> cells) co-expressed AR at the same levels (**Figure 4o-u**). However, there  
180 were sex-specific differences observed as greater percentage of *Dbx1*-derived cells in males  
181 (26.8% $\pm$ 4.1) expressed AR than *Dbx1*-derived cells in females (8.4% $\pm$ 3.6).

182 We also analyzed the contribution of the *Dbx1*-derived and Foxp2<sup>+</sup> populations to the  
183 total ER $\alpha$ , Aromatase and AR MeA populations (**Figure 4- Figure supplement 2**). We observed  
184 that both *Dbx1*-derived and Foxp2<sup>+</sup> cells comprised between ~10 to 22% of the total ER $\alpha$   
185 population in male and female mice. The *Dbx1*-derived population contributed between ~30-  
186 40% of the total aromatase population in males and females, which was significantly greater than  
187 the contribution of the Foxp2<sup>+</sup> population in both males and females. *Dbx1*-derived (males only)  
188 and Foxp2<sup>+</sup> cells (males and females) comprised ~20-38% of the total AR<sup>+</sup> population. In  
189 contrast, the *Dbx1*-derived population contributed to only 3% of the total AR<sup>+</sup> population in  
190 females, which was significantly less than the Foxp2<sup>+</sup> contribution in females and less than the  
191 contribution of *Dbx1*-derived cells in males. Collectively, these data reveal that *Dbx1*-derived  
192 and Foxp2<sup>+</sup> cells contributed differentially to the aromatase and AR populations, but not to the  
193 ER $\alpha$  population.

194

195 *Sex-specific subtype activation patterns during innate behaviors*

196 The MeA receives direct inputs from the accessory olfactory bulb (AOB) (Scalia, Winans 1975,  
197 Martel, Baum 2009, Bergan, Ben-Shaul & Dulac 2014) and integrates this chemosensory  
198 information to regulate innate behaviors including territorial aggression, maternal aggression,  
199 mating, and predator avoidance (Dulac, Wagner 2006, Kim et al. 2015). Previous data revealed  
200 that at least aggressive and mating behaviors are controlled by MeA GABAergic neurons (Choi  
201 et al. 2005, Hong, Kim & Anderson 2014). However, whether different subsets of inhibitory  
202 neurons are activated during these behaviors, or if neuronal subtype activation is generalizable  
203 across behaviors remains unknown. To directly test these possibilities we performed well  
204 characterized aggression, mating and predator odor avoidance behavioral tests in both male and  
205 female resident mice and examined the patterns of activation of *Dbx1*-derived and *Foxp2*<sup>+</sup> cells  
206 using c-fos as a readout of neuronal activity in resident mice (**Figure 5- Figure supplement 1**).

207

208 *Dbx1-derived and Foxp2<sup>+</sup> neurons are activated during aggressive encounters*

209 To evaluate activation of *Dbx1*-derived and *Foxp2*<sup>+</sup> neurons during male conspecific aggression,  
210 we performed a territorial aggression assay in which an intruder mouse was placed in a resident  
211 cage. Concordant with previous literature (Wang et al. 2013), we found a significant increase in  
212 the number of c-fos<sup>+</sup> cells in the MeA in comparison to naïve mice (**Figure 5a-c**). In addition,  
213 both the number and proportion of activated *Dbx1*-derived and *Foxp2*<sup>+</sup> subpopulations in males  
214 were significantly increased during territorial aggression compared to control (naïve) mice  
215 (**Figure 5d-k, x**). We next evaluated aggression in female mice by conducting a maternal  
216 aggression assay in which pups were removed from a nursing female and a sexually naïve male  
217 intruder was introduced (Haney, DeBold & Miczek 1989). In addition to the naïve control, we

218 established a second control in which pups were removed and no intruder was presented. With  
219 this control, we could compare levels of neuronal activation during maternal aggression (pups  
220 removed and presence of intruder) to levels of neuronal activation in response to a strong stressor  
221 (pups removed but no intruder) and to a naïve condition (with pups and without intruder). We  
222 found a significant increase in the number of c-fos<sup>+</sup> cells in the MeA in the maternal aggression  
223 condition compared to both stressed and naïve controls (**Figure 5l-o**). When examining subtype  
224 specific levels of activation, we found that both the number and proportion of activated *Dbx1*-  
225 derived and the *Foxp2*<sup>+</sup> subpopulations significantly increased during maternal aggression in  
226 comparison to the naïve condition (**Figure 5p-w, y**). Thus, during an aggressive encounter with  
227 a conspecific, both *Dbx1*-derived and *Foxp2*<sup>+</sup> MeA subpopulations were activated to a greater  
228 extent in both male and female mice..

229

### 230 *Dbx1*-derived and *Foxp2*<sup>+</sup> neurons are activated in a sex-specific manner during mating

231 We next conducted male and female mating assays and monitored animals for mating (mounting  
232 and intromission followed by presence of a vaginal plug). Consistent with previous studies  
233 (Rowe, Erskine 1993), we observed an increase in c-fos<sup>+</sup> cells in the MeA during both male and  
234 female mating (**Figure 6a-c**). Intriguingly, we found subpopulation specific differences in  
235 activation patterns across sexes. While the number and proportion of the activated *Dbx1*-derived  
236 subpopulation was significantly increased during both male and female mating when compared  
237 to naïve controls (**Figure 6d-g, l**), the number and proportion of activated *Foxp2*<sup>+</sup> cells increased  
238 only during male but not during female mating (**Figure 6h-k, m**). Thus, while *Dbx1*-derived and  
239 *Foxp2*<sup>+</sup> MeA subpopulations were both activated during male mating, only *Dbx1*-derived  
240 neurons were activated during female mating.

241

242 *Activation of Dbx1-derived and Foxp2+ neurons during predator odor exposure*

243 We next sought to determine whether *Dbx1*-derived and Foxp2+ MeA subpopulations were  
244 activated by a strong innate stressor. To accomplish this, we exposed mice to rat odor, a well-  
245 characterized predator cue that evokes a strong aversive response in mice (Apfelbach et al. 2005,  
246 Carvalho et al. 2015). Mice were exposed to soiled bedding from a rat cage (predator) or clean  
247 bedding (benign) as a control (**Figure 7**). Consistent with previous studies (Canteras, Pavesi &  
248 Carobrez 2015), in response to predator odor we observed a significant increase in the number of  
249 c-fos+ cells in the MeA in both male and female mice (**Figure 7a-c**). Interestingly, the *Dbx1*-  
250 derived cells in male and female mice were not activated in response to predator odor exposure  
251 in comparison to the benign bedding (**Figure 7d-g**). In contrast, we observed a significant  
252 activation of Foxp2+ cells in comparison to controls in female mice, but not in males (**Figure**  
253 **7h-k**). When we assessed percentage of both *Dbx1*-derived (YFP+;c-fos+/total YFP+) and  
254 Foxp2+ (Foxp2+;c-fos+/total Foxp2+) cells co-labeled with c-fos over the total population there  
255 was no significant difference either subpopulation nor in male or female mice compared to  
256 control (**Figure 7m-l**). This suggests that despite an increase in the number of activated Foxp2+  
257 cells in female mice in the presence of rat bedding, this increase might not be physiologically  
258 relevant. Therefore, to investigate which MeA subpopulation may be responding to predator  
259 odor, we next examined the activation patterns of the OTP+ population. We observed that a  
260 greater number of OTP+ cells in both males and females were activated in response to predator  
261 odor (**Figure 7- Figure supplement 1**). When analyzing the proportion of OTP+ cells activated,  
262 we found no differences between the benign and the predator avoidance groups in males, but we  
263 did find a significant increase in the OTP+ population in females. Therefore, in the female brain,

264 the OTP+ population, in contrast to *Dbx1*-derived or *Foxp2*+ cells, were activated at a level  
265 above control in response to a strong aversive innate olfactory cue.

266 In summary, our analyses of activation patterns in response to a battery of innate  
267 behavior tasks revealed that *Dbx1*-derived and *Foxp2*+ cells in the MeA were differentially  
268 activated depending on the instinctive behavioral task (**Figure 8**). The most striking of these  
269 differences occurred during mating behaviors. While both subpopulations were activated during  
270 male mating, in the female MeA only *Dbx1*-derived neurons were activated, with no activation  
271 of the *Foxp2*+ population. In contrast, the OTP+ population in females appears more tuned to a  
272 predator odor cue. Importantly, sex differences in patterns of neuronal activation during mating  
273 and predator odor were not due to overall differences in the activation of the MeA as these cues  
274 activated the MeA in both sexes. Taken together with our electrophysiological and molecular  
275 findings of the *Dbx1*-derived and *Foxp2*+ populations, our data reveal that developmental  
276 parcellation of MeA progenitors predicts mature neuronal identity and sex-specific innate  
277 behavioral activation patterns.

278

## 279 **Discussion**

280 Across a variety of species, innate behaviors such as aggression, mating and avoidance of  
281 predators are initiated by sensory cues primarily detected by olfaction (Dulac, Wagner 2006,  
282 Stowers, Cameron & Keller 2013). Here, focusing on the medial amygdala (MeA), a critical  
283 brain region for the processing of olfactory-based sensory cues for unlearned behavior in  
284 vertebrates, we took a neural developmental approach to shed light on how innate behavioral  
285 information may be encoded in the male and female brain. Integrating genetic fate-mapping,  
286 patch clamp electrophysiology and animal behavioral assays we uncover a fundamental link

287 between embryonic patterning and brain responses to innate behavioral cues at two levels: 1)  
288 differential transcription factor expression within the embryonic MeA progenitor niche predicts  
289 mature output neuronal subtype identity and 2) further predicts subpopulation sex-specific  
290 responses to mating and predator odor avoidance cues. Our findings further suggest that  
291 transcription factor expression at the progenitor stage may be instructive for establishment of  
292 neuronal populations and sub-circuits regulating sex-specific behaviors.

293

#### 294 **Potential transcription factor codes for establishment of MeA neuronal diversity**

295 The generation of neuronal diversity across amygdala subnuclei has been posited to occur in a  
296 compartmentalized manner with amygdala inhibitory neurons generated in the subpallial  
297 ganglionic eminences and excitatory neurons arising from the cortical pallial region (Swanson,  
298 Petrovich 1998). In this model, the amygdala and cerebral cortex develop by a similar  
299 mechanism with neurons in both structures originating in shared progenitor domains. However,  
300 more recent studies have revealed that generation of amygdala neuronal diversity is more  
301 complex with large populations of neurons originating in progenitor niches dedicated for limbic  
302 structures (Remedios et al. 2007, Hirata et al. 2009, Soma et al. 2009, Waclaw et al. 2010,  
303 Garcia-Moreno et al. 2010). One of these major niches encompasses the region at the  
304 telencephalic-diencephalic border, an origin of MeA output neurons (Hirata et al. 2009, Garcia-  
305 Moreno et al. 2010). Our previous studies revealed that the homedomain encoding transcription  
306 factor, *Dbx1*, marks a subpopulation of progenitors within the POA, which will later generate a  
307 subset of MeA inhibitory output neurons (Hirata et al. 2009). Here, we significantly extend this  
308 work by revealing the presence of a complementary population of progenitors within this niche  
309 marked by expression of *Foxp2*. Thus, our findings, combined with previous work, suggest a



310 model of MeA development in which distinct progenitor populations at the telencephalic-  
311 diencephalic border defined by differential transcription factor expression (e.g. *Dbx1*, *Foxp2*,  
312 *OTP*) are a major source for MeA neuronal diversity.

313         The function of combinatorial sets of transcription factors in neural progenitors has been  
314 shown across the neuraxis as the mechanism for the generation and specification of distinct  
315 subclasses of neurons (Kepecs, Fishell 2014, Stepien, Tripodi & Arber 2010, Shirasaki, Pfaff  
316 2002). In addition to specification of neuronal subtype identity, recent studies in the spinal cord  
317 and globus pallidus (Dodson et al. 2015, Bikoff et al. 2016) have revealed that different  
318 combinatorial codes in progenitor pools predict neuronal subtype connectivity patterns, neuronal  
319 firing properties and in the case of the globus pallidus, distinct functions in regulating voluntary  
320 movements (Dodson et al. 2015). Thus, transcription factor expression at the earliest stages of  
321 neuronal development likely represents the beginning of an instructive continuum for the  
322 establishment of not only neuronal identity, but also development of sub-circuitry regulating  
323 different components of motor behaviors. Here, we show that in the MeA, complementary  
324 transcription factor expression marks subsets of progenitors and predicts neuronal subtype  
325 identity as defined by molecular and electrophysiological signatures. At the molecular level,  
326 *Dbx1*-derived and *Foxp2*<sup>+</sup> neurons express different combinations of the sex steroid hormone  
327 pathway protein aromatase and estrogen receptor alpha (*ER* $\alpha$ ). At the electrophysiological level,  
328 these two populations possess distinct intrinsic electrophysiological profiles. Thus, our study  
329 generates a novel cell-specific transcription factor-based means to predict postnatal MeA  
330 neuronal identity.

331

332 **Behavioral activation of *Dbx1*-derived and *Foxp2*<sup>+</sup> neurons**

333 The central importance of the MeA for processing innate behaviors such as aggression, mating  
334 and predator avoidance is well-established (Dulac, Wagner 2006, Sokolowski, Corbin 2012).  
335 Despite this knowledge, the question of which MeA neuronal subtypes encode instinctive  
336 behavioral information has only recently begun to be addressed. Recent optogenetic  
337 manipulation of the MeA revealed that glutamatergic neurons mediate repetitive self-grooming  
338 behaviors while in contrast GABA-ergic neurons regulate either aggressive or mating behaviors,  
339 depending on the level of neuronal activity driven by light stimulation (Hong, Kim & Anderson  
340 2014). Moreover, MeA neuronal subclasses expressing different components of the stress  
341 response system control appropriate behavioral responses to social cues (Shemesh et al. 2016).  
342 Here, we contribute to the understanding of amygdala cell-specific regulation of behavior by  
343 generating a transcription factor based map of MeA subtype responsiveness to innate-behavioral  
344 cues. Thus, our findings provide a developmental molecular context in which to further dissect  
345 neuronal subtype control of MeA-driven behaviors.

346 In addition to playing a central role in processing sensory information required for  
347 instinctive behaviors, the MeA is one of the known sexually dimorphic structures of the brain  
348 (Cooke, Woolley 2005, McCarthy, Arnold 2011, Johnson, Breedlove & Jordan 2008). Recent  
349 studies employing *in vivo* recording techniques revealed that a significant number of MeA  
350 neurons are dedicated to processing olfactory cues from the opposite sex rather than the same-  
351 sex, thus providing a direct demonstration of sex-specific differences in sensory processing  
352 (Bergan, Ben-Shaul & Dulac 2014). However, the identity of male and female MeA neurons that  
353 differentially process olfactory-based sensory information has not been delineated. Here, we  
354 reveal that while *Dbx1*-derived and *Foxp2*<sup>+</sup> neurons are broadly activated by mating, aggressive  
355 and predator cues, we found stark differences in *Dbx1*-derived, *Foxp2*<sup>+</sup> and *OTP*<sup>+</sup> cell-specific

356 responses in the male and female brain to mating and predator odor cues. A similar sex-specific  
357 control of innate behavior has been directly demonstrated in the ventromedial hypothalamus  
358 (VMH), where progesterone receptor-expressing neurons while required for male aggressive and  
359 mating behaviors, are only required for female mating behavior (Yang et al. 2013). Collectively,  
360 our studies in combination with previous studies point to a larger picture in which there are  
361 neuronal subpopulations in the MeA and VMH that are involved in the regulation of different  
362 innate behaviors in a sex-specific manner.

363         Although our data do not reveal the neuronal and/or circuit mechanisms underlying our  
364 observation of sex-specific subpopulation responses to mating behavior and predator odor  
365 presentation, some of our findings do provide potential insight as to how this differential  
366 processing may occur. The two most straightforward and non-exclusive potential mechanisms  
367 are: 1) with regard to mating, intrinsic differences in *Dbx1*-derived and *Foxp2*<sup>+</sup> neurons and/or  
368 2) subpopulation specific patterns of local and/or long-range connectivity.

369         Regarding the first potential mechanism, sex steroid hormones and receptors such as  
370 aromatase, ER $\alpha$  and AR have been extensively characterized as critical for the output of distinct  
371 components of male and female aggressive and mating behaviors (Yang, Shah 2014). For  
372 example, deletion of AR resulted in alterations in attack duration during territorial aggression  
373 and initiation of male mating (Juntti et al. 2010), while ablation of aromatase neurons led to  
374 impairments in the production of distinct components of aggression in male and female mice  
375 (Unger et al. 2015). Consistent with the critical role that these factors play in components of  
376 innate behaviors, we found that aromatase is expressed solely in the *Dbx1*-derived lineage.  
377 Across species, aromatase has a masculinizing effect (Wu et al., 2009; Balthazart et al. 2011)

378 Thus, it will be interesting to explore how *Dbx1*-derived aromatase expressing neurons may  
379 control male behavioral displays such as mounting and territorial aggression.

380 Furthermore, both *Dbx1*-derived and *Foxp2*<sup>+</sup> neurons possess distinct  
381 electrophysiological profiles, another potential mechanism to control different components of  
382 behaviors. Previous work in both vertebrates and invertebrates has revealed that the timing of AP  
383 spiking is directly linked to specific behavioral actions. For example, in vertebrates timescale  
384 firing differences are associated with dopamine (DA) release for the determination of reward  
385 behaviors (Schultz 2007, Zhang et al. 2009). It will therefore prove interesting to explore if and  
386 how firing patterns of *Dbx1*-derived and *Foxp2*<sup>+</sup> MeA neurons may control different  
387 components of innate behaviors across sexes.

388 The second potential and perhaps more intriguing mechanism that may account for *Dbx1*-  
389 derived and *Foxp2*<sup>+</sup> subtype specific male versus female patterns of neuronal activation during  
390 mating are sex specific local and/or long-range patterns of connectivity. Although currently not  
391 yet observed in a brain circuit in mammals, such a mechanism has recently been uncovered in *c.*  
392 *elegans* in which shared male and female circuits show differences in connectivity that is  
393 established during wiring (Oren-Suissa, Bayer & Hobert 2016). Consistent with this, there is  
394 some suggestion of sex-specific differences in olfactory-MeA projections in rodents (Kang et al.  
395 2011). Although we did not differentiate according to sex of the animal, we found differences in  
396 both the amplitude and frequency of EPSCs between lineages, indicating differences in the  
397 strength and/or number of inputs between *Dbx1*-derived and *Foxp2*<sup>+</sup> MeA neurons. Although the  
398 source of input cannot be determined from our analysis, there are direct excitatory inputs to the  
399 MeA emanating from the mitral/tufted neurons of the accessory olfactory bulb (AOB) (Martel,

400 Baum 2009, Bergan, Ben-Shaul & Dulac 2014). Thus, determination of input/output wiring  
401 patterns of male and female *Dbx1*-derived and *Foxp2*<sup>+</sup> MeA neurons will be highly informative.

402 In summary, although the precise instructive developmental mechanisms programming  
403 innate behaviors remain to be elucidated, we reveal that differential transcription factor  
404 expression during development is predictive of neuronal identity based on molecular and  
405 electrophysiological criteria and sex-specific patterns of neuronal activation during innate  
406 behaviors.

407

## 408 **Methods**

### 409 *Animals*

410 Mice were housed in the temperature and light-controlled (12h light-dark cycle) Children's  
411 National Medical Center animal care facility and given food and water *ad libitum*. All animal  
412 procedures were approved by the Children's National Medical Center's Institutional Animal  
413 Care and Use Committee (IACUC) and conformed to NIH Guidelines for animal use. Mice used  
414 were *Dbx1cre*<sup>+/+</sup> (kindly provided by A. Peirani, Institut Jacques Monod, Paris), *Shhcre*<sup>+/+</sup>  
415 (Jackson Labs strain B6.Cg-*Shhtm1(EGFP/cre)Cjt/J*), *Emx1cre*<sup>+/+</sup> (Jackson Labs strain  
416 B6.129S2-*Emx1tm1(cre)Krl/J*), *Nkx6.2cre*<sup>+/+</sup> (Jackson Lab strain Tg *Nkx6-2-*  
417 *icre)1Kess/Sshi/J*), *Foxp2cre*<sup>+/+</sup> (kindly provided by R. Palmiter, University of Washington)  
418 (Roussio et al. 2016), all crossed to *Rosa26YFP*<sup>+/+</sup> mice (Jackson lab strain R26R-EYFP). For  
419 analysis of aromatase expression, we used Aromatase LacZ reporter mice (kindly provided by N.  
420 Shah, University of California-San Francisco) (Wu et al. 2009). Mice were genotyped by  
421 Transnetyx Inc. Genotyping Services. Adult mice were considered between 3-7 months of age.

422 Sample size was based on previous experiments and published data. No statistical methods were  
423 used to determine sample sizes.

424

#### 425 ***Immunohistochemistry***

426 Postnatal mice were transcardially perfused with 4% paraformaldehyde (PFA) and brains post  
427 fixed overnight at 4°C, embedded in 4% agarose (Invitrogen) and sectioned at 50 µm with a  
428 vibrating microtome (Leica VT1000S). Embryos were fixed in 4% PFA overnight at 4°C  
429 degrees, cryoprotected in 30% sucrose, embedded in O.C.T. compound (Tekka) and sectioned at  
430 20 µm on a cryostat (Leica CM1850). For IHC, tissue sections were incubated overnight with  
431 primary antibody, then washed with PBST and 10% normal donkey serum and incubated for 4  
432 hours with the corresponding secondary antibodies, and mounted with DAPI Fluoromount  
433 (SouthernBiotech 0100-20). Primary antibodies used were rat anti-GFP (to detect YFP  
434 expression, (1:1000, Nacalai 04404-84), goat anti-Foxp2 (1:200; Santa Cruz sc-21069), rabbit  
435 anti-Foxp2 (1:500; abcam ab16046), rabbit anti-OTP (1:2000; kind provided by F. Vaccarino,  
436 Yale University), rabbit anti-androgen receptor (1:750; Epitomics AC-0071), rabbit anti-estrogen  
437 receptor  $\alpha$  (1:6000; Millipore 06-935); mouse anti-NeuN (1:200; Millipore MAB-377), mouse  
438 anti-CC1 (1:250; Calbiochem OP80-100), goat anti-calbindin (1:200; Santa Cruz sc-7691), rat  
439 anti-somatostatin (1:100; Millipore MAB354), rabbit anti-cfos (1:500; Santa Cruz sc-52), goat  
440 anti-cfos (1:300; Santa Cruz sc-52G), anti-rabbit nNOS (1:8000; ImmunoStar 24287), mouse  
441 anti-CAMKII $\alpha$  (1:500 Biomol ARG22260.50) and chicken anti- $\beta$ Gal (1:2000; abcam 9361).  
442 Secondary antisera used were donkey anti-rat or anti-goat Alexa 488 (1:200; Life Technologies),  
443 anti-rabbit or anti-goat Cy5 (1:1000; Jackson ImmunoResearch), anti-rabbit or anti-mouse Cy3

444 (1:1000; Jackson ImmunoResearch), anti-mouse dylight 649 (1:500; Jackson ImmunoResearch),  
445 or anti-chicken dylight 549 (1:500; Jackson ImmunoResearch).

446

#### 447 *Microscopy*

448 Fluorescent photographs were taken using an Olympus FX1000 Fluoview Laser Scanning  
449 Confocal Microscope (1µm optical thickness)

450

#### 451 *Quantification*

##### 452 *Molecular marker analysis*

453 For embryonic analysis, the average of 2-3 sections encompassing the POA were imaged and  
454 quantified (**Figure 1; Figure 1-Figure supplement 1-2**). For adult analyses (**Figures 1-7;**  
455 **Figure 1- Figure supplement 1-2; Figure 2- Figure supplement 1; Figure 4-Figure**  
456 **supplement 1; Figure 5- Figure supplement 1; Figure 7-Figure supplement 1**), every 6<sup>th</sup>  
457 serial coronal section encompassing the anterior to posterior extent of the MeA (Bregma -1.30 to  
458 -1.90, see **Figure 1- Figure supplement 3**) was immunostained with antibodies to Foxp2, YFP  
459 and markers of interest. Quantification was done by counting single and double-labeled cells  
460 encompassing the entire domain of expression within the POA or MeA (**Figures 1-2, 4; Figure**  
461 **1- Figure supplement 1-2; Figure 2- Figure supplement 1; Figure 4-Figure supplement 1**).

462

##### 463 *Neuronal activation*

464 For analyses of neuronal activation (**Figures 5-7, Figure 7- Figure supplement 1**), a single  
465 MeA section with highest number of c-fos<sup>+</sup> cells corresponding with the presence of *Dbx1*-  
466 derived, Foxp2<sup>+</sup> or OTP<sup>+</sup> cells was chosen for quantification. c-fos, YFP and Foxp2 triple

467 immunostaining was conducted on the same section and single and double labeled cells counted.  
468 c-fos and OTP double immunostaining was conducted and single and double cells counted.

469

#### 470 *Statistical Evaluation*

471 Unless otherwise stated, data was analyzed using GraphPad 6 statistical software. We first tested  
472 the distribution of the data with the Shapiro-Wallis test for normality. Data that was normally  
473 distributed was analyzed using an unpaired two-tailed *t*-test for analysis of experiments involving  
474 two groups (**Figure 1-Figure supplement 1; Figure 1- Figure supplement 2; Figure 5x;**  
475 **Figure 6c females, k, m, l; Figure 7c, g males, k, l, m Foxp2+ subpopulation; Figure 7-**  
476 **Figure supplement 1c, d, h, i)** and a one-way ANOVA (**Figure 5o, w, y Foxp2+**  
477 **subpopulation)** followed by Tukey-Kramer multiple comparison test was used for analysis of  
478 experiments involving three or more groups. Data with a non-normal distribution was analyzed  
479 by using the non-parametric test Mann-Whitney when comparing two groups (**Figure 5c, g, k, y**  
480 **Dbx1-derived subpopulation; Figure 6c males, g; Figure 7g females, m Dbx1-derived**  
481 **subpopulation; Figure 7-Figure supplement 1j, k)** and Kruskal-Wallis with Dunn's post-hoc  
482 corrections for data with three groups (**Figure 5s**). For analysis of data shown in **Figure 4** and  
483 **Figure 4- Figure supplement 1** we performed the following statistical analysis: when the data  
484 met the normality assumption or could be transformed to meet the normality assumption,  
485 generally two-way analysis of variance models were implemented to evaluate the evidence of  
486 differences in mean effects of the two experimental factors on cell activation (**Figure 4 g, u;**  
487 **Figure 4-Figure supplement 2 a, b**). In the situation where no data transformation could be  
488 found to achieve an acceptable level of normality, quantile regression was performed, which  
489 does not require the normality assumption, to evaluate comparable differences in median effects



490 **(Figure 4 n; Figure 4-Figure supplement 2c)**. In each case, the initial models included a cross-  
491 products term to assess evidence of effect modification or interaction. When there was no  
492 interaction, it was taken as evidence of the absence of effect modification and the cross-products  
493 term was removed leaving only a model that assessed independent effects of the each factor  
494 separately, while holding constant any effects of the other factor. Depending on the underlying  
495 model, either mean or median effects +/- 95% confidence intervals were derived to reflect  
496 differences that were consistent with statistically meaningful differences in the final  
497 model. Under consideration of protecting the experiment-wise error rate, as long as the  
498 evaluation of differences focused only on identifying the nature of effects deemed statistically  
499 meaningful in the final model, there was no correction made for multiple comparisons. Analysis  
500 of data meeting the normality assumption was based on GraphPad Prism 6 and analysis based on  
501 quantile regression was implemented in Stata 13. As mice had to be sacrificed after each  
502 behavioral assay in order to conduct c-fos immuno-analysis, technical repeats were not available.  
503 Measurements from different mice were considered biological repeats to determine sample size.  
504 Data points were considered outliers and excluded if they were two standard deviations away  
505 from the mean.

506

### 507 *Electrophysiology and biocytin filling*

508 Mice (P25-40) were anaesthetized with isoflurane and sacrificed. Brains were removed and  
509 immediately immersed in ice-cold oxygenated (95% O<sub>2</sub>/5% CO<sub>2</sub>) sucrose solution (234 mM  
510 sucrose, 11 mM glucose, 26 mM NaHCO<sub>3</sub>, 2.5 mM KCl, 1.25 mM NaH<sub>2</sub>PO<sub>4</sub>·H<sub>2</sub>O, 10 mM  
511 MgSO<sub>4</sub> and 0.5 mM CaCl<sub>2</sub>). Coronal slices of 300µm in thickness were cut. Slices with  
512 amygdala were collected and placed in oxygen-equilibrated artificial cerebral spinal fluid

513 (ACSF) as previously described (Hirata et al. 2009). Either *Dbx1*-derived or *Foxp2*-derived  
514 neurons were then visualized using a fluorescent lamp (Nikon) with a 450-490 $\lambda$  filter. Whole-  
515 cell patch-clamp recordings from YFP-positive fluorescent cells were performed at room  
516 temperature with continuous perfusion of ACSF (Multiclamp 700A, DigiDATA1322, Molecular  
517 Devices). Intracellular solution (in mM): 130 Kgluconate, 10 KCl, 2 MgCl<sub>2</sub>, 10 HEPES, 10  
518 EGTA, 2 Na<sub>2</sub>-ATP, 0.5 Na<sub>2</sub>-GTP. All measurements of intrinsic and synaptic properties were  
519 analyzed off-line using Clampfit Software (V.10.2, Molecular Devices) and graphing software  
520 (OriginPro 9.1). At the end of each recording, biocytin (1%) was injected with the depolarizing  
521 current (1nA) for post-hoc morphology analysis. All slices were then fixed with  
522 paraformaldehyde overnight at 4°C and processed for Fluorescein-conjugated Avidin-D (1:200,  
523 Vector Laboratories), YFP IHC (*Dbx1*-derived and *Foxp2*<sup>+</sup> recordings) or *Foxp2* IHC (for  
524 *Foxp2*<sup>+</sup> recordings) as described above.

525

### 526 ***Neuronal Reconstruction***

527 Neurons were filled with biocytin and imaged using an Olympus FX1000 Fluoview Laser  
528 Scanning Confocal Microscope (0.5 $\mu$ m optical thickness). VIAS software was used to align  
529 confocal images taken at 40x and 60x in the same plane (x,y,z). Neurons were then traced using  
530 neuTube software, which uses fixed radii small tubes to estimate the dendritic branches length  
531 and thickness (Feng, Zhao & Kim 2015).

532

### 533 ***Behavioral assays***

534 *Dbx1cre*<sup>+/+</sup>; *Rosa26YFP*<sup>+/+</sup> male and female mice 3-7 months old were used for the behavioral  
535 assays. One week prior to testing, animals were single housed. Testing was performed between

536 the hours of 18:00 and 20:00 corresponding to the beginning of the dark cycle for all assays  
537 except the maternal aggression assay which took place from 13:00 to 15:00pm corresponding to  
538 the light cycle.

539

#### 540 *Mating*

541 Sexually naïve hormonally primed females were analyzed during female mating. Mating was  
542 assessed by placing a mouse of the opposite sex inside the resident's cage and checking for plugs  
543 every 30 minutes. When a plug was observed, noting successful intromission, female or male  
544 mate was removed from the cage and the experimental animal was left inside the cage for an  
545 additional 30 minutes before being sacrificed. Females with no plugs were excluded from the  
546 analysis as no mating occurred.

547

#### 548 *Territorial and maternal aggression*

549 Male territorial aggression was assessed by performing a resident-intruder assay in which an  
550 unfamiliar male mouse ('intruder') was placed inside the resident's cage for 10 minutes. During  
551 this period, the homecage male displayed typical aggressive behaviors including attacking and  
552 biting. The intruder was removed and the after an additional 50 minutes the resident male was  
553 sacrificed. For the maternal aggression assay, female mice were single-housed after a plug was  
554 observed. The following experimental conditions were run: 1) for maternal aggression pups age  
555 between P5-P8 were removed and 2 minutes later a sexually naïve male was introduced into the  
556 cage for 10 minutes, 2) for 'no pups' condition, pups were removed but no intruder presented  
557 and 3) for naïve control, the cage was undisturbed in which pups were not removed and no  
558 intruder presented. In conditions 1) & 2) the female mice were sacrificed after 50 minutes after

559 pup removal. If female mice did not actively attack the intruder at least two times, they were  
560 excluded from the analysis. All male mice attacked the intruder for the 10 minute period.

561

#### 562 *Predator avoidance*

563 Predator avoidance was assessed by introducing a petri dish containing rat bedding to the  
564 homecage for 1 hour. The control predator group was presented with a petri dish containing  
565 clean mouse bedding (benign). Mice were sacrificed after 1 hour presentation of rat bedding or  
566 benign bedding. Mice that did not show escaping responses after the presentation of the petri  
567 dish were excluded.

#### 568 **Acknowledgements**

569 We thank V. Gallo, J. Triplett and I. Zohn for constructive input and/or critical reading of the  
570 manuscript. We also thank members of the Corbin and Triplett labs for input during the course of  
571 this study and Robert McCarter, Director of the DC- IDDRC Biostatistics and Informatics Core  
572 for his expert biostatistics assistance. We thank A. Pierini for *Dbx1<sup>cre</sup>* mice, R. Palmiter for  
573 *Foxp2<sup>cre</sup>* mice sent prior to publication (Rousso et al. 2016), N. Shah for *AromataseLacZ* reporter  
574 mice, and F. Vaccarino for the OTP antibody. This work was partially supported by NIH grants  
575 R01 NIDA020140 (J.G.C), and R01 DC012050 (J.G.C). Core support was provided by the  
576 CNMC DC-IDDRC Imaging, Biostatistics and Informatics and Animal Neurobehavior  
577 Evaluation Cores (NIH IDDRC P30HD040677). J.E.L. is a predoctoral student in the Molecular  
578 Medicine Program of the Institute for Biomedical Sciences at The George Washington  
579 University. This work is from a dissertation to be presented to the above program in partial  
580 fulfillment of the requirements for the Ph.D. degree.

581 **References**

- 582 Apfelbach, R., Blanchard, C.D., Blanchard, R.J., Hayes, R.A. & McGregor, I.S. 2005, "The effects of  
583 predator odors in mammalian prey species: a review of field and laboratory studies", *Neuroscience*  
584 *and biobehavioral reviews*, vol. 29, no. 8, pp. 1123-1144.
- 585 Bale, T.L. & Epperson, C.N. 2015, "Sex differences and stress across the lifespan", *Nature neuroscience*,  
586 vol. 18, no. 10, pp. 1413-1420.
- 587 Balthazart, J., Charlier, T.D., Cornil, C.A., Dickens, M.J., Harada, N., Konkle, A.T.M., Voigt, C. & Ball,  
588 G.F. 2011. "Sex differences in brain aromatase activity: genomic and non-genomic controls",  
589 *Frontiers in Endocrinology*, vol. 2, no. 34.
- 590 Bergan, J.F., Ben-Shaul, Y. & Dulac, C. 2014, "Sex-specific processing of social cues in the medial  
591 amygdala", *eLife*, vol. 3, pp. e02743.
- 592 Bian, X. 2013, "Physiological and morphological characterization of GABAergic neurons in the medial  
593 amygdala", *Brain research*, vol. 1509, pp. 8-19.
- 594 Bikoff, J.B., Gabitto, M.I., Rivard, A.F., Drobac, E., Machado, T.A., Miri, A., Brenner-Morton, S.,  
595 Famojure, E., Diaz, C., Alvarez, F.J., Mentis, G.Z. & Jessell, T.M. 2016, "Spinal Inhibitory  
596 Interneuron Diversity Delineates Variant Motor Microcircuits", *Cell*, vol. 165, no. 1, pp. 207-219.
- 597 Canteras, N.S., Pavesi, E. & Carobrez, A.P. 2015, "Olfactory instruction for fear: neural system analysis",  
598 *Frontiers in neuroscience*, vol. 9, pp. 276.
- 599 Carney, R.S., Mangin, J.M., Hayes, L., Mansfield, K., Sousa, V.H., Fishell, G., Machold, R.P., Ahn, S.,  
600 Gallo, V. & Corbin, J.G. 2010, "Sonic hedgehog expressing and responding cells generate neuronal  
601 diversity in the medial amygdala", *Neural development*, vol. 5, pp. 14-8104-5-14.
- 602 Carvalho, V.M., Nakahara, T.S., Cardozo, L.M., Souza, M.A., Camargo, A.P., Trintinalia, G.Z., Ferraz,  
603 E. & Papes, F. 2015, "Lack of spatial segregation in the representation of pheromones and  
604 kairomones in the mouse medial amygdala", *Frontiers in neuroscience*, vol. 9, pp. 283.
- 605 Choi, G.B., Dong, H.W., Murphy, A.J., Valenzuela, D.M., Yancopoulos, G.D., Swanson, L.W. &  
606 Anderson, D.J. 2005, "Lhx6 delineates a pathway mediating innate reproductive behaviors from the  
607 amygdala to the hypothalamus", *Neuron*, vol. 46, no. 4, pp. 647-660.
- 608 Cooke, B.M. & Woolley, C.S. 2005, "Sexually dimorphic synaptic organization of the medial amygdala",  
609 *The Journal of neuroscience : the official journal of the Society for Neuroscience*, vol. 25, no. 46,  
610 pp. 10759-10767.
- 611 Dodson, P.D., Larvin, J.T., Duffell, J.M., Garas, F.N., Doig, N.M., Kessar, N., Duguid, I.C., Bogacz, R.,  
612 Butt, S.J. & Magill, P.J. 2015, "Distinct developmental origins manifest in the specialized encoding  
613 of movement by adult neurons of the external globus pallidus", *Neuron*, vol. 86, no. 2, pp. 501-513.
- 614 Dulac, C. & Wagner, S. 2006, "Genetic analysis of brain circuits underlying pheromone signaling",  
615 *Annual Review of Genetics*, vol. 40, pp. 449-467.

- 616 Erskine, M.S. 1993, "Mating-induced increases in FOS protein in preoptic area and medial amygdala of  
617 cycling female rats", *Brain research bulletin*, vol. 32, no. 5, pp. 447-451.
- 618 Feng, L., Zhao, T. & Kim, J. 2015, "neuTube 1.0: A New Design for Efficient Neuron Reconstruction  
619 Software Based on the SWC Format", *eNeuro*, vol. 2, no. 1, pp. 10.1523/ENEURO.0049-14.2014.  
620 eCollection 2015 Jan-Feb.
- 621 Flames, N., Pla, R., Gelman, D.M., Rubenstein, J.L., Puelles, L. & Marin, O. 2007, "Delineation of  
622 multiple subpallial progenitor domains by the combinatorial expression of transcriptional codes",  
623 *The Journal of neuroscience : the official journal of the Society for Neuroscience*, vol. 27, no. 36,  
624 pp. 9682-9695.
- 625 Fogarty, M., Grist, M., Gelman, D., Marin, O., Pachnis, V., & Kessar, N. 2007, "Spatial genetic  
626 patterning of the embryonic neuroepithelium generates GABAergic interneuron diversity in the adult  
627 cortex", *Journal of Neuroscience*, vol 27, no. 41, pp. 10935-10946.
- 628 French, C.A. & Fisher, S.E. 2014, "What can mice tell us about Foxp2 function?", *Current opinion in  
629 neurobiology*, vol. 28, pp. 72-79.
- 630 Garcia-Moreno, F., Pedraza, M., Di Giovannantonio, L.G., Di Salvio, M., Lopez-Mascaraque, L.,  
631 Simeone, A. & De Carlos, J.A. 2010, "A neuronal migratory pathway crossing from diencephalon to  
632 telencephalon populates amygdala nuclei", *Nature neuroscience*, vol. 13, no. 6, pp. 680-689.
- 633 Gorski, J.A., Talley, T., Qiu, M., Puelles, L., Rubenstein, J.L.R. & Jones, K.R. 2002, "Cortical excitatory  
634 neurons and glia, but not GABAergic neurons, are produced in the Emx1-expressing lineage.", *The  
635 Journal of neuroscience*, vol. 22, no. 15, pp. 6309-6314.
- 636 Gross, C.T. & Canteras, N.S. 2012, "The many paths to fear", *Nature reviews.Neuroscience*, vol. 13, no.  
637 9, pp. 651-658.
- 638 Haney, M., DeBold, J.F. & Miczek, K.A. 1989, "Maternal aggression in mice and rats towards male and  
639 female conspecifics.", *Aggressive Behavior*, vol. 15, pp. 443-453.
- 640 Hirata, T., Li, P., Lanuza, G.M., Cocas, L.A., Huntsman, M.M. & Corbin, J.G. 2009, "Identification of  
641 distinct telencephalic progenitor pools for neuronal diversity in the amygdala.", *Nature  
642 Neuroscience*, vol. 12, no. 2, pp. 141-149.
- 643 Hong, W., Kim, D. & Anderson, D. 2014, "Antagonistic Control of Social versus Repetitive Self-  
644 Grooming Behaviors by Separable Amygdala Neuronal Subsets", *Cell*, vol. 158, no. 6, pp. 1348-  
645 1361.
- 646 Johnson, R.T., Breedlove, S.M. & Jordan, C.L. 2008, "Sex differences and laterality in astrocyte number  
647 and complexity in the adult rat medial amygdala", *The Journal of comparative neurology*, vol. 511,  
648 no. 5, pp. 599-609.
- 649 Jones E.G., Huntley, G.W., Benson, D.L. 1994. "Alpha calcium/calmodulin-dependent protein kinase II  
650 selectively expressed in a subpopulation of excitatory neurons in monkey sensory-motor cortex:  
651 comparison with GAD-67 expression", *Journal of Neuroscience*, vol 14, pp.611-629.

- 652 Juntti, S.A., Tollkuhn, J., Wu, M.V., Fraser, E.J., Soderborg, T., Tan, S., Honda, S., Harada, N. & Shah,  
653 N.M. 2010, "The Androgen Receptor Governs the Execution, but Not Programming, of Male Sexual  
654 and Territorial Behaviors", *Neuron*, vol. 66, no. 2, pp. 260-272.
- 655 Kang, N., McCarthy, E.A., Cherry, J.A. & Baum, M.J. 2011, "A sex comparison of the anatomy and  
656 function of the main olfactory bulb-medial amygdala projection in mice", *Neuroscience*, vol. 172,  
657 pp. 196-204.
- 658 Kepecs, A. & Fishell, G. 2014, "Interneuron cell types are fit to function", *Nature*, vol. 505, no. 7483, pp.  
659 318-326.
- 660 Keshavarzi, S., Sullivan, R.K., Ianno, D.J. & Sah, P. 2014, "Functional properties and projections of  
661 neurons in the medial amygdala", *The Journal of neuroscience : the official journal of the Society for*  
662 *Neuroscience*, vol. 34, no. 26, pp. 8699-8715.
- 663 Kim, Y., Venkataraju, K.U., Pradhan, K., Mende, C., Taranda, J., Turaga, S.C., Arganda-Carreras, I., Ng,  
664 L., Hawrylycz, M.J., Rockland, K.S., Seung, H.S. & Osten, P. 2015, "Mapping social behavior-  
665 induced brain activation at cellular resolution in the mouse", *Cell reports*, vol. 10, no. 2, pp. 292-  
666 305.
- 667 Koenning, M., Jackson, S., Hay, C.M., Faux, C., Kilpatrick, T.J., Willingham, M. & Emery, B. 2012,  
668 "Myelin gene regulatory factor is required for maintenance of myelin and mature oligodendrocyte  
669 identity in the adult CNS", *The Journal of neuroscience : the official journal of the Society for*  
670 *Neuroscience*, vol. 32, no. 36, pp. 12528-12542.
- 671 Kollack, S.S. & Newman, S.W. 1992, "Mating behavior induces selective expression of Fos protein  
672 within the chemosensory pathways of the male Syrian hamster brain", *Neuroscience letters*, vol. 143,  
673 no. 1-2, pp. 223-228.
- 674 Kondo, Y. 1992, "Lesions of the medial amygdala produce severe impairment of copulatory behavior in  
675 sexually inexperienced male rats", *Physiology & Behavior*, vol. 51, no. 5, pp. 939-943.
- 676 Llinas, R.R. 1988, "The intrinsic electrophysiological properties of mammalian neurons: insights into  
677 central nervous system function", *Science (New York, N.Y.)*, vol. 242, no. 4886, pp. 1654-1664.
- 678 Martel, K.L. & Baum, M.J. 2009, "A centrifugal pathway to the mouse accessory olfactory bulb from the  
679 medial amygdala conveys gender-specific volatile pheromonal signals", *The European journal of*  
680 *neuroscience*, vol. 29, no. 2, pp. 368-376.
- 681 McCarthy, M.M. & Arnold, A.P. 2011, "Reframing sexual differentiation of the brain", *Nature*  
682 *neuroscience*, vol. 14, no. 6, pp. 677-683.
- 683 Mullen, R.J., Buck, C.R. & Smith, A.M. 1992, "NeuN, a neuronal specific nuclear protein in vertebrates",  
684 *Development (Cambridge, England)*, vol. 116, no. 1, pp. 201-211.
- 685 Oren-Suissa, M., Bayer, E.A. & Hobert, O. 2016, "Sex-specific pruning of neuronal synapses in  
686 *Caenorhabditis elegans*", *Nature*, vol. 533, no. 7602, pp. 206-211.

- 687 Petilla Interneuron Nomenclature Group, Ascoli, G.A., Alonso-Nanclares, L., Anderson, S.A.,  
688 Barrionuevo, G., Benavides-Piccione, R., Burkhalter, A., Buzsaki, G., Cauli, B., Defelipe, J., Fairen,  
689 A., Feldmeyer, D., Fishell, G., Fregnac, Y., Freund, T.F., Gardner, D., Gardner, E.P., Goldberg, J.H.,  
690 Helmstaedter, M., Hestrin, S., Karube, F., Kisvarday, Z.F., Lambolez, B., Lewis, D.A., Marin, O.,  
691 Markram, H., Munoz, A., Packer, A., Petersen, C.C., Rockland, K.S., Rossier, J., Rudy, B.,  
692 Somogyi, P., Staiger, J.F., Tamas, G., Thomson, A.M., Toledo-Rodriguez, M., Wang, Y., West, D.C.  
693 & Yuste, R. 2008, "Petilla terminology: nomenclature of features of GABAergic interneurons of the  
694 cerebral cortex", *Nature reviews.Neuroscience*, vol. 9, no. 7, pp. 557-568.
- 695 Remedios, R., Huilgol, D., Saha, B., Hari, P., Bhatnagar, L., Kowalczyk, T., Hevner, R.F., Suda, Y.,  
696 Aizawa, S., Ohshima, T., Stoykova, A. & Tole, S. 2007, "A stream of cells migrating from the  
697 caudal telencephalon reveals a link between the amygdala and neocortex", *Nature neuroscience*, vol.  
698 10, no. 9, pp. 1141-1150.
- 699 Rousso, D.L., Qiao, M., Kagan, R.D., Yamagata, M., Palmiter, R.D. & Sanes, J.R. 2016, "Two Pairs of  
700 ON and OFF Retinal Ganglion Cells Are Defined by Intersectional Patterns of Transcription Factor  
701 Expression", *Cell reports*, vol. 15, no. 9, pp. 1930-1944.
- 702 Rowe, D.W. & Erskine, M.S. 1993, "c-Fos proto-oncogene activity induced by mating in the preoptic  
703 area, hypothalamus and amygdala in the female rat: role of afferent input via the pelvic nerve",  
704 *Brain research*, vol. 621, no. 1, pp. 25-34.
- 705 Scalia, F. & Winans, S.S. 1975, "The differential projections of the olfactory bulb and accessory olfactory  
706 bulb in mammals", *The journal of comparative neurology*, vol. 161, no. 1, pp. 31-55.
- 707 Schultz, W. 2007, "Multiple dopamine functions at different time courses", *Annual Review of*  
708 *Neuroscience*, vol. 30, pp. 259-288.
- 709 Shemesh, Y., Forkosh, O., Mahn, M., Anpilov, S., Sztainberg, Y., Manashirov, S., Shlapobersky, T.,  
710 Elliott, E., Tabouy, L., Ezra, G., Adler, E.S., Ben-Efraim, Y.J., Gil, S., Kuperman, Y., Haramati, S.,  
711 Dine, J., Eder, M., Deussing, J.M., Schneidman, E., Yizhar, O. & Chen, A. 2016, "Ucn3 and CRF-  
712 R2 in the medial amygdala regulate complex social dynamics", *Nature neuroscience*, .
- 713 Shirasaki, R. & Pfaff, S.L. 2002, "Transcriptional codes and the control of neuronal identity", *Annual*  
714 *Review of Neuroscience*, vol. 25, pp. 251-281.
- 715 Sokolowski, K. & Corbin, J.G. 2012, "Wired for behaviors: from development to function of innate  
716 limbic system circuitry", *Frontiers in molecular neuroscience*, vol. 5, pp. 55.
- 717 Sokolowski, K., Esumi, S., Hirata, T., Kamal, Y., Tran, T., Lam, A., Oboti, L., Brighthaupt, S.C.,  
718 Zaghulula, M., Martinez, J., Ghimbovschi, S., Knoblach, S., Pierani, A., Tamamaki, N., Shah, N.M.,  
719 Jones, K.S. & Corbin, J.G. 2015, "Specification of select hypothalamic circuits and innate behaviors  
720 by the embryonic patterning gene *dbx1*", *Neuron*, vol. 86, no. 2, pp. 403-416.
- 721 Soma, M., Aizawa, H., Ito, Y., Maekawa, M., Osumi, N., Nakahira, E., Okamoto, H., Tanaka, K. &  
722 Yuasa, S. 2009, "Development of the mouse amygdala as revealed by enhanced green fluorescent  
723 protein gene transfer by means of in utero electroporation", *The Journal of comparative neurology*,  
724 vol. 513, no. 1, pp. 113-128.



- 725 Stepien, A.E., Tripodi, M. & Arber, S. 2010, "Monosynaptic rabies virus reveals premotor network  
726 organization and synaptic specificity of cholinergic partition cells", *Neuron*, vol. 68, no. 3, pp. 456-  
727 472.
- 728 Stowers, L., Cameron, P. & Keller, J.A. 2013, "Ominous odors: olfactory control of instinctive fear and  
729 aggression in mice", *Current opinion in neurobiology*, vol. 23, no. 3, pp. 339-345.
- 730 Swanson, L.W. & Petrovich, G.D. 1998, "What is the amygdala?", *Trends in neurosciences*, vol. 21, no.  
731 8, pp. 323-331.
- 732 Takahashi, L.K. & Gladstone, C.D. 1988, "Medial amygdaloid lesions and the regulation of sociosexual  
733 behavioral patterns across the estrous cycle in female golden hamsters", *Behavioral neuroscience*,  
734 vol. 102, no. 2, pp. 268-275.
- 735 Tanaka, M., Ikeda, T., Hayashi, S., Iijima, N., Amaya, F., Hisa, Y., Ibata, Y. 1997, "Nitroergic  
736 neurons in the medial amygdala project to the hypothalamic paraventricular nucleus of the  
737 rat" *Brain Research*, vol 777, pp. 13-21.
- 738 Unger, E.K., Burke, K.J., Jr, Yang, C.F., Bender, K.J., Fuller, P.M. & Shah, N.M. 2015, "Medial  
739 amygdalar aromatase neurons regulate aggression in both sexes", *Cell reports*, vol. 10, no. 4, pp.  
740 453-462.
- 741 Vochtelloo, J.D. & Koolhaas, J.M. 1987, "Medial amygdala lesions in male rats reduce aggressive  
742 behavior: interference with experience", *Physiology & Behavior*, vol. 41, no. 2, pp. 99-102.
- 743 Waclaw, R.R., Ehrman, L.A., Pierani, A. & Campbell, K. 2010, "Developmental origin of the neuronal  
744 subtypes that comprise the amygdalar fear circuit in the mouse", *The Journal of neuroscience : the  
745 official journal of the Society for Neuroscience*, vol. 30, no. 20, pp. 6944-6953.
- 746 Wang, Y., He, Z., Zhao, C. & Li, L. 2013, "Medial amygdala lesions modify aggressive behavior and  
747 immediate early gene expression in oxytocin and vasopressin neurons during intermale exposure",  
748 *Behavioural brain research*, vol. 245, pp. 42-49.
- 749 Wu, M.V., Manoli, D.S., Fraser, E.J., Coats, J.K., Tollkuhn, J., Honda, S., Harada, N. & Shah, N.M.  
750 2009, "Estrogen masculinizes neural pathways and sex-specific behaviors", *Cell*, vol. 139, no. 1, pp.  
751 61-72.
- 752 Yang, C.F. & Shah, N.M. 2014, "Representing sex in the brain, one module at a time.", *Neuron*, vol. 82,  
753 no. 2, pp. 261-278.
- 754 Yang, C.F., Chiang, M.C., Gray, D.C., Prabhakaran, M., Alvarado, M., Juntti, S.A., Unger, E.K., Wells,  
755 J.A. & Shah, N.M. 2013, "Sexually dimorphic neurons in the ventromedial hypothalamus govern  
756 mating in both sexes and aggression in males", *Cell*, vol. 153, no. 4, pp. 896-909.
- 757 Zhang, L., Doyon, W.M., Clark, J.J., Phillips, P.E. & Dani, J.A. 2009, "Controls of tonic and phasic  
758 dopamine transmission in the dorsal and ventral striatum", *Molecular pharmacology*, vol. 76, no. 2,  
759 pp. 396-404.

760 Zhao, T., Szabo, N., Ma, J., Luo, L., Zhou, X. & Alvarez-Bolado, G. 2008, "Genetic mapping of Foxb1-  
761 cell lineage shows migration from caudal diencephalon to telencephalon and lateral hypothalamus",  
762 *The European journal of neuroscience*, vol. 28, no. 10, pp. 1941-1955.

763

764

765

766 **Figure Legends**

767 **Figure 1. Embryonic and postnatal segregation of *Dbx1*-derived and *Foxp2*<sup>+</sup> cells.**

768 Minimal co-localization of *Dbx1*-derived (green) and *Foxp2*<sup>+</sup> (red) labeled cells in coronal  
769 sections at the level of the POA at E11.5 (a-f) and E13.5 (g-l). As shown at E11.5 (s) *Foxp2*<sup>+</sup>  
770 precursors in the VZ (arrows) are observed putatively migrating to the SVZ. The segregation of  
771 *Dbx1*-derived and *Foxp2*<sup>+</sup> cells persists into adulthood (m-r). Summary schematic of spatial  
772 segregation of *Dbx1*-derived and *Foxp2*<sup>+</sup> cells in the embryonic POA and postnatal MeA (t).  
773 Venn diagram depicting the overlap of the total number of *Dbx1*-derived and *Foxp2*<sup>+</sup> cells in 2-3  
774 sections/embryo or 5-8 sections/adult brain. The scale bars represent 200µm (a-c, g-i, s), 100µm  
775 (m-o) and 25µm (d-f, j-l, p-r). Abbreviations: MeA, medial amygdala; MePD, medial amygdala-  
776 posterior dorsal; MePV, medial amygdala posterior ventral; POA, preoptic area; SVZ,  
777 subventricular zone; V, ventricle; VZ, ventricular zone. *n*=3 embryonic brains; *n*=5 postnatal  
778 brains. Data are mean  $\pm$  s.e.m. *n* is the number of animals.

779

780 **Figure 2. Identity of *Foxp2*<sup>+</sup> medial amygdala neurons.**

781 Dual immunofluorescence of *Foxp2* with NeuN (*n*=3 mice) (a-d), CC1 (*n*=3 mice) (e-h), YFP  
782 (in *Emx1<sup>cre</sup>;RYFP* mice) (*n*=5 mice) (i-l), calbindin (*n*=3 mice) (m-p), nNOS (*n*=6 mice) (q-t),  
783 and somatostatin (*n*=4 mice) (u-x) (arrows show double labeled cells). Quantification of co-  
784 localization with each marker (y). Data are mean  $\pm$  s.e.m. *n* is the number of animals. The scale  
785 bar represents 200µm (a, e, i, m, q, u) and 25µm (b-d, f-h, j-l, n-p, r-t, v-x).

786

787 **Figure 3. *Dbx1*-derived and *Foxp2*<sup>+</sup> MeA neurons possess distinct electrophysiological**  
788 **properties.**

789 Typical firing patterns of *Dbx1*-derived (a) and *Foxp2*<sup>+</sup> (b) neurons with current injections at -  
790 60pA, +20pA and +60pA. Significant differences across populations in resting membrane  
791 potential (*R<sub>m</sub>*) (c), voltage at rest (*V<sub>rest</sub>*) (d), capacitance (e), and action potential (AP) firing  
792 patterns (f) but not rheobase (g) are observed (two-tailed *t*-test, (c) *p*=0.0006, *t*=3.676, *df*=49; (d)  
793 *p*=0.036, *t*=2.159, *df*=49; (e) *p*=0.002, *t*=3.1987, *df*=49; (f) *p*=0.016, *t*=3.1988, *df*=49; (g)  
794 *p*=0.610, *t*=0.514, *df*=49; *n*=28 *Dbx1*-derived cells and *n*=23 *Foxp2*<sup>+</sup> cells). Excitatory post-  
795 synaptic currents (EPSCs) are observed in both *Dbx1*-derived (h) and *Foxp2*<sup>+</sup> (i) neurons, with  
796 significant differences in sEPSC frequency (j), amplitude (k) and decay (l) (two-tailed *t*-test, (j)  
797 *p*<0.0001, *t*=3.041, *df*= 34; (k) *p*=0.006, *t*=2.949, *df*=34; (l) *p*=0.005, *t*=3.041, *df*=34; *n*=28  
798 *Dbx1*-derived neurons, *n*=23 *Foxp2*<sup>+</sup> neurons). Data are mean ± s.e.m. *n* is the number of cells.  
799 *p*<0.05 (\*), *p*<0.01 (\*\*), and *p*<0.001 (\*\*\*), n.s.; not significant.

800

801 **Figure 4. Expression of sex hormone pathway markers in *Dbx1*-derived and *Foxp2*<sup>+</sup> cells.**

802 Dual immunofluorescence for YFP (green) or *Foxp2* (red) with the sex steroid hormone pathway  
803 markers (white): estrogen receptor  $\alpha$  (ER $\alpha$ ) (a-g), aromatase (h-n) or androgen receptor (AR) (o-  
804 u) (arrows show double labeled cells). Subpopulations of both *Dbx1*-derived (a-c, g) and *Foxp2*<sup>+</sup>  
805 cells express ER $\alpha$  (d-g). Quantification reveals a greater percentage of *Dbx1*-derived cells  
806 expressing ER $\alpha$  compared to *Foxp2*<sup>+</sup> cells in females (two-way ANOVA with no interaction  
807 between subpopulation and sex, but with main effect for subpopulation *p*=0.0433,  
808 *F*(1,10)=5.352; *n*=4 and *x*=45.38 for *Dbx1*-derived cells in female mice, *n*=4 and *x*=24.77 for  
809 *Foxp2*<sup>+</sup> cells in female mice, *n*=3 and *x*=28.43 for *Dbx1*-derived cells in male mice, *n*=3 and  
810 *x*=24 for *Foxp2*<sup>+</sup> cells in male mice). The majority of *Dbx1*-derived cells express aromatase in  
811 both males and females (h-j, n). In contrast, only a small percentage of *Foxp2*<sup>+</sup> cells in both

812 males express aromatase (two quantile regression analysis for non-normal distributions shows no  
813 interaction for sex and subpopulation but a main effect for subpopulation  $p=0.000$  with a 95%  
814 confidence interval of 31.27 and 69.53,  $n=3$  for *Dbx1*-derived cells in male mice,  $n=3$  and for  
815 *Foxp2*<sup>+</sup> cells in male mice,  $n=3$  for mice for *Dbx1*-derived cells in female mice,  $n=3$  and for  
816 *Foxp2*<sup>+</sup> female mice). A greater percentage of *Dbx1*-derived neurons in males express AR in  
817 comparison to *Dbx1*-derived cells in female mice (o-q, u). No differences in percentages of  
818 *Foxp2*<sup>+</sup> male or female subpopulations expressing AR (r-u) nor differences across  
819 subpopulations (two-way ANOVA with no interaction between subpopulation and sex, but with  
820 main effect for sex  $p=0.0166$ ,  $F(1,8)=9.118$ ;  $n=3$  and  $x=10.07$  for *Dbx1*-derived cells in female  
821 mice,  $n=3$  and  $x=7.133$  for *Foxp2*<sup>+</sup> cells in female mice,  $n=3$  and  $x=24.3$  for *Dbx1*-derived cells  
822 in male mice,  $n=3$  and  $x=16.27$  for *Foxp2*<sup>+</sup> cells in male mice). Data are mean  $\pm$  s.e.m.  $n$  is the  
823 number of animals and  $x$  is the mean. The scale bar represents 50 $\mu$ m.  $p<0.05$  (\*) and  $p<0.01$   
824 (\*\*).

825

826 **Figure 5. *Dbx1*-derived and *Foxp2*<sup>+</sup> neurons are activated during aggressive encounters.**

827 Significant increases in the number of c-fos<sup>+</sup> cells (white) compared to controls is observed in  
828 the MeA during both male territorial aggression (a-c) (two tailed Mann-Whitney test,  $U=0$ ,  
829  $p=0.0025$ ,  $n=5$  naïve mice,  $n=7$  territorial aggression) and maternal aggression (one-way  
830 ANOVA,  $p<0.0001$ ,  $F(2, 18)=19.05$ ,  $n=7$  naïve mice,  $n=6$  ‘no pup’ condition,  $n=8$  maternal  
831 aggression) (l-o). Dual immunofluorescence for c-fos (white) and YFP (green) or *Foxp2* (red)  
832 after male territorial aggression reveals an increase in the number of *Dbx1*-derived cells (two-  
833 tailed Mann-Whitney test,  $U=4$ ,  $p=0.0238$ ,  $n= 6$ ) (d-g) and *Foxp2*<sup>+</sup> cells (two-tailed Mann-  
834 Whitney test,  $U=0$ ,  $p=0.0023$   $n=7$ ) expressing c-fos in comparison to naïve control mice ( $n=6$ )

835 not exposed to an intruder (h-k). In female mice, an increase in the number *Dbx1*-derived cells  
836 expressing c-fos during maternal aggression ( $n=4$ ) in comparison to naïve ( $n=5$ ), but not in the  
837 ‘no pups’ conditions ( $n=4$ ), is observed (Kruskal-Wallis test,  $X^2(3,13)=7.124$   $p=0.0164$ ) (p-s).  
838 There is also an increase in the number of Foxp2+ cells ( $n=8$ ) expressing c-fos during maternal  
839 aggression in comparison to the naïve ( $n=7$ ) and ‘no pups’ control conditions ( $n=6$ ) (one-way  
840 ANOVA  $p<0.0001$ ,  $F(2,18)=16.93$ ) (t-w). Analyses of the percentage of both *Dbx1*-derived  
841 (YFP+ and c-fos+ /total YFP+) and Foxp2+ cells (Foxp2+ and c-fos+ / total Foxp2+) expressing  
842 c-fos in male mice reveals an increase in both the *Dbx1*-derived subpopulation ( $n=6$ ) (two-tailed  
843 *t*-test,  $p=0.0009$ ,  $t=4.685$ ,  $df=11$ ) and the Foxp2+ subpopulation ( $n=7$ ) (two-tailed *t*-test,  
844  $p=0.001$ ,  $t=4.295$ ,  $df=11$ ) in comparison to naïve controls ( $n=6$ ) (x). In females, the percentage of  
845 *Dbx1*-derived cells expressing c-fos during maternal aggression is higher in comparison to the  
846 naïve condition but not to the ‘no pups’ condition (Kruskal-Wallis test,  $X^2(3,13)=9.461$   
847  $p=0.0005$ ,  $n=5$  naïve,  $n=4$  ‘no pups’ and  $n=4$  aggression) (y). The percentage of Foxp2+ cells  
848 expressing c-fos during maternal aggression is also higher during maternal aggression ( $n=8$ ) in  
849 comparison to both the naïve ( $n=7$ ) and ‘no pups’ ( $n=6$ ) controls (one way ANOVA,  $p<0.0001$ ,  
850  $F(2,18)=24.16$ ) (y). Data are mean  $\pm$  s.e.m.  $n$  is the number of animals. Arrows show double  
851 labeled cells.  $p<0.05$  (\*),  $p<0.01$  (\*\*), and  $p<0.001$  (\*\*\*). The scale bar represents 50 $\mu$ m.

852

### 853 **Figure 6. Sex-specific subpopulation responses during mating.**

854 A significant increase in the number of c-fos+ cells (white) in the MeA during mating compared  
855 to naïve control is observed in both male (two tailed Mann-Whitney test,  $U=0$ ,  $p=0.0079$ ,  $n=5$   
856 naïve,  $n=5$  mating) and female brains (two-tailed *t*-test,  $p=0.0038$ ,  $t=4.022$ ,  $df=8$ ,  $n=6$  naïve,  $n=4$   
857 mating) (a-c). Double immunofluorescence for c-fos (white) and YFP (green) or Foxp2 (red)

858 after mating reveals an increase in the number of *Dbx1*-derived neurons expressing c-fos in male  
859 (two tailed Mann-Whitney test,  $U=2$ ,  $p=0.0152$ ,  $n=6$  naïve,  $n=5$  mating) and female (two tailed  
860 Mann-Whitney test,  $U=1$ ,  $p=0.0476$ ,  $n=6$  naïve,  $n=3$  mating) brains (d-g). A significant increase  
861 in the number of Foxp2+ cells expressing c-fos is only observed in male mice during mating  
862 (two-tailed *t*-test,  $p=0.009$ ,  $t=3.331$ ,  $df=9$ ,  $n=6$  naïve,  $n=5$  mating) but not in female mice during  
863 mating (two tailed *t*-test,  $p=0.8993$ ,  $t=0.1312$ ,  $df=7$ ,  $n=6$  naïve,  $n=3$  mating) as compared to  
864 naïve controls (h-k). A significant increase in the percentage of *Dbx1*-derived cells expressing c-  
865 fos (YFP+ and c-fos+ /total YFP+) is observed in males during mating in comparison to the  
866 naïve controls (two-tailed *t*-test,  $p=0.0067$ ,  $t=3.507$ ,  $df=9$ ,  $n=6$  naïve,  $n=5$  mating) (m). A  
867 significant increase in the percentage of Foxp2+ cells expressing c-fos (Foxp2+ and c-fos+ /total  
868 Foxp2+) in male brains during mating is also observed in comparison to naïve controls (two-  
869 tailed *t*-test,  $p=0.0001$ ,  $t=6.477$ ,  $df=9$ ,  $n=6$  naïve,  $n=5$  mating) (m). An increase in the percentage  
870 of *Dbx1*-derived cells expressing c-fos (two-tailed *t*-test,  $p=0.0131$ ,  $t=3.302$ ,  $df=7$ ,  $n=6$  naïve,  
871  $n=3$  mating) is observed in female brains during mating (l). In contrast, no increase is observed  
872 in the Foxp2+ population (two-tailed *t*-test,  $p=0.0905$ ,  $t=1.96$ ,  $df=7$ ,  $n=6$  naïve,  $n=3$  mating) in  
873 female brains during mating (l). Data are mean  $\pm$  s.e.m. *n* is the number of animals.  $p<0.05$  (\*),  
874  $p<0.01$  (\*\*), and  $p<0.001$  (\*\*\*), n.s.; not significant. Arrows show double labeled cells. The  
875 scale bar represents 50 $\mu$ m.

876

877 **Figure 7. *Dbx1*-derived and Foxp2+ MeA subpopulation activation patterns in response to**  
878 **predator odor.**

879 A significant increase in the number of c-fos+ cells (white) in the MeA in both male (two-tailed  
880 *t*-test,  $p=0.0344$ ,  $t=0.3.153$ ,  $df=4$ ,  $n=3$  benign,  $n=3$  predator avoidance) and female (two-tailed *t*-

881 test,  $p=0.001$ ,  $t=4.778$ ,  $df=9$ ,  $n=6$  benign,  $n=5$  predator avoidance) brains is observed in the  
882 presence of rat bedding compared to benign unsoiled bedding (a-c). Double immunofluorescence  
883 for c-fos (white) and YFP (green) or Foxp2 (red) after predator odor exposure reveals no  
884 increase in the number of *Dbx1*-derived cells (two-tailed *t*-test,  $p=0.687$ ,  $t=0.35$ ,  $df=4$ ,  $n=3$   
885 benign,  $n=3$  predator avoidance) (d-g) or Foxp2<sup>+</sup> cells (two-tailed *t*-test,  $p=0.703$ ,  $t=0.70$ ,  $df=4$ ,  
886  $n=3$  benign,  $n=3$  predator avoidance) (h-k) expressing c-fos in male brains as compared to  
887 control. In the female brain, there is also no increase in the number of *Dbx1*-derived cells during  
888 predator odor exposure as compared to control (two tailed Mann-Whitney,  $U=5$ ,  $p=0.1349$ ,  $n=5$   
889 benign,  $n=5$  predator avoidance) (d-g). In contrast, an increase the number of Foxp2<sup>+</sup> cells (two-  
890 tailed *t*-test,  $p=0.036$ ,  $t=2.47$ .  $df=9$ ,  $n=6$  benign,  $n=5$  predator avoidance) in female brains is  
891 observed (h-k). Analysis of the percentage of *Dbx1*-derived (YFP<sup>+</sup> and c-fos<sup>+</sup> /total YFP<sup>+</sup>) and  
892 Foxp2<sup>+</sup> cells (Foxp2<sup>+</sup> and c-fos<sup>+</sup> / total Foxp2<sup>+</sup>) expressing c-fos in both male and female brains  
893 revealed no increases in either population (*Dbx1*-derived population in male mice: two-tailed *t*-  
894 test,  $p=0.2318$ ,  $t=1.408$ ,  $df=4$ , naïve  $n=3$ , predator avoidance  $n=3$ ; Foxp2<sup>+</sup> population in male  
895 mice: two-tailed *t*-test,  $p=0.1023$ ,  $t=2.11$ ,  $df=4$ , naïve  $n=3$ , predator avoidance  $n=3$ ; *Dbx1*-  
896 derived population in female mice: two-tailed Mann-Whitney,  $U=5$ ,  $p=0.1349$ , naïve  $n=5$ ,  
897 predator avoidance  $n=5$ ; Foxp2<sup>+</sup> population in female mice: two-tailed *t*-test,  $p=0.2299$ ,  $t=1.288$ ,  
898  $df=9$ , naïve  $n=6$ , predator avoidance  $n=5$ ). Data are mean  $\pm$  s.e.m.  $n$  is the number of animals.  
899 Arrows show double labeled cells.  $p<0.05$  (\*),  $p<0.01$  (\*\*), and  $p<0.001$  (\*\*\*). The scale bar  
900 represents 50 $\mu$ m.

901

902 **Figure 8. Summary of findings.**



903 Schematic summarizing our findings in which embryonic segregation of *Dbx1*-derived (green)  
904 and *Foxp2*<sup>+</sup> (red) cells in the embryonic brain predicts postnatal intrinsic electrophysiological  
905 profiles and differential sex and subpopulation-specific neuronal activation patterns (neurons  
906 indicate activation and X's indicate no activation) in response to aggression (territorial and  
907 maternal), mating and predator avoidance. The OTP<sup>+</sup> population is shown responding to  
908 predator odor in female brains. The male predator odor responsive population remains to be  
909 determined.

910

## 911 **Supplemental Figures**

912

### 913 **Figure 1- Figure supplement 1. Embryonic and postnatal distribution of OTP<sup>+</sup> cells.**

914 Dual immunostaining of coronal sections at the telencephalic-diencephalic border at E11.5  
915 shows very little overlap between *Dbx1*-derived (green) (*n*=3) and the *Foxp2*<sup>+</sup> (red) (*n*=3)  
916 progenitor populations with the OTP<sup>+</sup> population (white) (a-f). Quantification of overlap of  
917 OTP with the *Dbx1*-derived and *Foxp2*<sup>+</sup> populations (YFP<sup>+</sup> and OTP<sup>+</sup>/ total YFP<sup>+</sup> population  
918 for *Dbx1*-derived cells; *Foxp2*<sup>+</sup> OTP<sup>+</sup>/ total *Foxp2*<sup>+</sup> population for *Foxp2*<sup>+</sup> cells) (g). Venn  
919 diagrams depicting the overlap of the total number of *Dbx1*-derived (h) and *Foxp2*<sup>+</sup> cells (i) with  
920 the OTP<sup>+</sup> population (2-3 sections/embryo). Dual immunostaining of postnatal coronal sections  
921 also revealed very little overlap of *Dbx1*-derived population (*n*=3) or *Foxp2*<sup>+</sup> populations (*n*=4)  
922 with OTP (j-u). Quantification of overlap of OTP with the *Dbx1*-derived and *Foxp2*<sup>+</sup>  
923 populations (YFP<sup>+</sup> and OTP<sup>+</sup>/ total YFP<sup>+</sup> population for *Dbx1*-derived cells; *Foxp2*<sup>+</sup> OTP<sup>+</sup>/  
924 total *Foxp2*<sup>+</sup> population for *Foxp2*<sup>+</sup> cells) (v). Venn diagram depicting the overlap of the total  
925 number of *Dbx1*-derived (w) and *Foxp2*<sup>+</sup> cells (x) with the marker OTP<sup>+</sup> (average of MeA A-P

926 extent across 5-8 sections).  $p < 0.05$  (\*). The scale bar represents 100  $\mu\text{m}$  (a-f, j-l, p-r) and 100  $\mu\text{m}$   
927 (m-o, s-u). Data are mean  $\pm$  s.e.m.  $n$  is the number of animals.

928

929 **Figure 1- Figure supplement 2. Foxp2+ cells are not derived from the *Shh*- or *Nkx6.2***  
930 **lineages.**

931 Dual immunostaining of the amygdala primordium in horizontal sections at E11.5 reveals minor  
932 contribution of either the *Nkx6.2*-lineage ( $n=3$ ) (white) (a-d, i) or the *Shh*-lineage ( $n=3$ ) (white)  
933 (e-h, i) to the Foxp2+ population (red). Data are mean  $\pm$  s.e.m.  $n$  is the number of animals.  
934  $p < 0.05$  (\*). The scale bar represents 200 $\mu\text{m}$  (a, e) and 25  $\mu\text{m}$  (b-d, f-h).

935

936 **Figure 1- Figure supplement 3. Localization of *Dbx1*-derived and Foxp2+ cells in the adult**  
937 **MeA.**

938 Double immunofluorescence staining of adult coronal sections at the level of the MeA shows  
939 patterns of localization of *Dbx1*-derived (green) and Foxp2+ (red) cells across the anterior to  
940 posterior extent of the MeA (a-i). Bregma levels correspond to the K. Franklin and G. Paxinos  
941 Mouse Brain in Stereotaxic Coordinates Atlas. The scale bar represents 200 $\mu\text{m}$ .

942

943 **Figure 2- Figure supplement 1. Identity of OTP+ medial amygdala neurons.**

944 Dual immunofluorescence of Foxp2 with YFP (in *Emx1<sup>cre</sup>;RYFP* mice) ( $n=3$ ) (a-d), CAMKII $\alpha$   
945 ( $n=3$ ) (e-h), calbindin ( $n=3$ ) (i-l) and somatostatin ( $n=3$  mice) (m-p) (arrows show double  
946 labeled cells). Quantification reveals that most Foxp2+ are not *Emx1*-derived, nor express  
947 somatostatin, express to some extent CAMKII $\alpha$ , but are mainly Calbindin+ (q) Data are mean  $\pm$

948 s.e.m.  $n$  is the number of animals. The scale bar represents 100 $\mu$ m (a, e, i, m) and 25 $\mu$ m (b-d, f-h,  
949 j-l, n-p),.

950

951 **Figure 3- Figure supplement 1. Foxp2+ neurons possess projection neuronal morphology.**

952 Biocytin filling depicting the morphology of a typical Foxp2+ neuron possessing dendritic spines  
953 (a-b, arrow). Representative 3-D reconstruction of several Foxp2+ neurons (c-e). The scale bars  
954 represent 100 $\mu$ m (a) and 10 $\mu$ m (b).

955

956 **Figure 4- Figure supplement 1. Patterns of MeA expression of sex steroid hormone**  
957 **markers.**

958 Schematic of adult brain shows MeA (red box) (a). Immunostaining for ER $\alpha$  (b), aromatase (c)  
959 or AR (d) shows patterns of localization in the MeA. The scale bar represents 100 $\mu$ m.

960

961 **Figure 4- Figure supplement 2. Percent contribution of *Dbx1*-derived and Foxp2+ cells to**  
962 **sex steroid hormone marker populations.**

963 The percent contribution of *Dbx1*-derived cells and Foxp2+ cells in male and female brains to  
964 the ER $\alpha$ , Aromatase+ and Androgen Receptor+ populations are as follows: ER $\alpha$ + population:  
965 *Dbx1*-derived contribution: 18% $\pm$ 4.2 (male  $n=3$ ,  $x=18.37$ ), 21% $\pm$ 3.59 (female  $n=4$ ,  $x=20.75$ ).  
966 Foxp2+ contribution: 11% $\pm$ 2.72 (male  $n=3$ ,  $x=10.89$ ); 21% $\pm$ 3.0 (female  $n=4$ ,  $x=19.48$ ). No  
967 subpopulation or sex differences were observed (two-way ANOVA with no interaction between  
968 subpopulation and sex and no main effects (F(1,10)=0.8261  $p=0.3848$ ) (a). Aromatase+  
969 population: *Dbx1*-derived contribution: 37% $\pm$ 9.89 (male  $n=3$ ,  $x=37$ ), 34% $\pm$ 6.05 (female  $n=3$ ,  
970  $x=33.6$ ). Foxp2+ contribution: 0% $\pm$ 0.3 (male  $n=0.3$ ), 10% $\pm$ 5.49 (female  $n=3$ ,  $x=9.667$ ) (b). This

971 difference in expression was significant across subpopulations (two-way ANOVA with no  
972 interaction between subpopulation and sex, with a main effect for subpopulation  $p=0.0015$ ,  
973  $F(1,8)=22.33$ ). Androgen Receptor+ population: *Dbx1*-derived contribution: 36.7%±16.71 (male  
974  $n=3$ ,  $x=31.81$ ), 3%±2.0 (female  $n=3$ ,  $x=2.11$ ), *Foxp2*+ contribution: 27%±4.05 (male  $n=3$ ,  
975  $x=26.45$ ), 23%±0.85 (female  $n=3$ ,  $x=22.69$ ) (c). A two-way ANOVA revealed no interaction  
976 between subpopulation and sex; however the value was trending ( $p=0.0660$ ), with a main effect  
977 for sex within the *Dbx1*-derived subpopulation ( $p=0.0107$ ,  $F(1,8)=10.95$ ). As the interaction was  
978 trending, we also analyzed subpopulation differences and found significant increases in the  
979 percent of AR+ expressing *Foxp2*+ cells in comparison to the *Dbx1*-derived subpopulation in  
980 females ( $p=0.0308$ ,  $F(1,8)=6.85$ ) (c).  $n$  is the number of animals and  $x$  is the mean.  $p<0.05$  (\*),  
981  $p<0.01$  (\*\*), and  $p<0.001$  (\*\*\*)).

982

983 **Figure 5- Figure supplement 1. c-fos expression in the postero-medial (MeApd) and**  
984 **postero-ventral (MeApv) subnuclei during different innate behavioral assays.**

985 Immunofluorescence staining for c-fos after innate behavioral assays: territorial (c-d) and  
986 maternal (g-h) aggression, mating (g-h), predator avoidance (k-l) and their respective native (a-b)  
987 and benign (i-j) controls.

988

989 **Figure 7- Figure supplement 1. Sex-specific activation of OTP+ cells during predator**  
990 **avoidance.**

991 A significant increase in number of c-fos+ cells (white) in the MeA in males (two-tailed  $t$ -test,  
992  $p=0.0004$ ,  $t=5.435$ ,  $df=9$ ,  $n=6$  benign,  $n=5$  predator avoidance) (a-c) and in females (two-tailed  $t$ -  
993 test,  $p=0.0010$ ,  $t=5.08$ ,  $df=8$ ,  $n=5$  benign,  $n=5$  predator avoidance) (a-b, c) in the presence of rat

994 bedding compared to benign unsoiled bedding. Double immunofluorescence for c-fos (white)  
995 and OTP (pink) after predator odor exposure reveals an increase in number of cells expressing c-  
996 fos in the male OTP+ subpopulation (two-tailed *t*-test,  $p=0.023$ ,  $t=2.727$ ,  $df=9$ ,  $n=6$  benign,  $n=5$   
997 predator avoidance) (e-h) and in the female OTP+ subpopulation (two-tailed *t*-test,  $p<0.0001$ ,  
998  $t=11.09$ ,  $df=8$ ,  $n=5$  benign,  $n=5$  predator avoidance). There is no difference in the percentage of  
999 OTP+ cells expressing c-fos (OTP+c-fos+/total OTP) between benign ( $n=6$ ) and predator  
1000 avoidance ( $n=6$ ) conditions in males (two tailed Mann-Whitney test,  $U=9$ ,  $p=0.3290$ ) (j). In  
1001 contrast, there is a significant increase in the percent of OTP+ cells expressing c-fos between  
1002 benign ( $n=5$ ) and predator avoidance ( $n=5$ ) conditions in female brains (two tailed Mann-  
1003 Whitney test,  $U=0$ ,  $p=0.0079$ ,  $n=5$  benign,  $n=5$  predator avoidance condition).  $p<0.05$  (\*),  
1004  $p<0.01$  (\*\*), and  $p<0.001$  (\*\*\*)). Arrows show double labeled cells. The scale bar represents  
1005  $50\mu\text{m}$ .  
1006

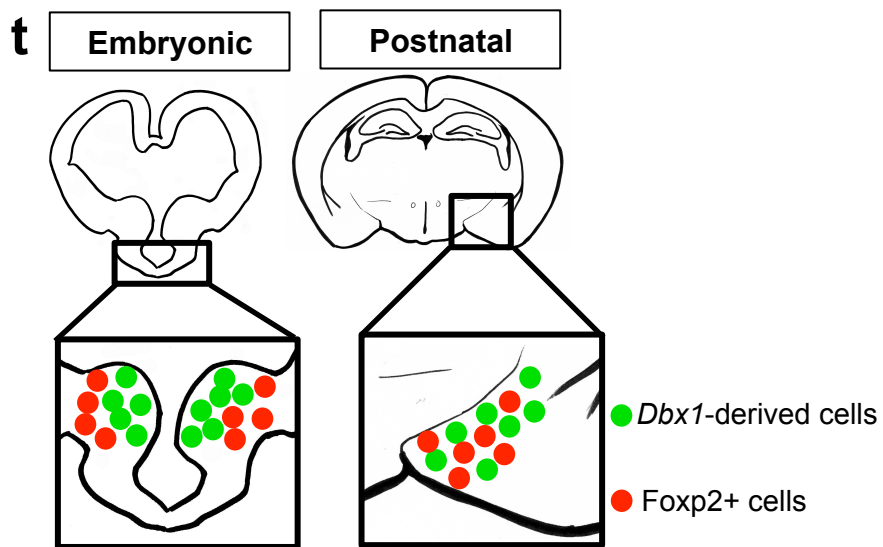
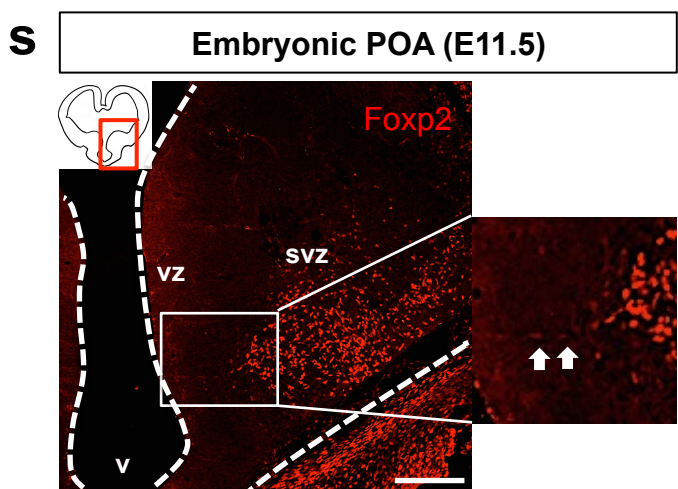
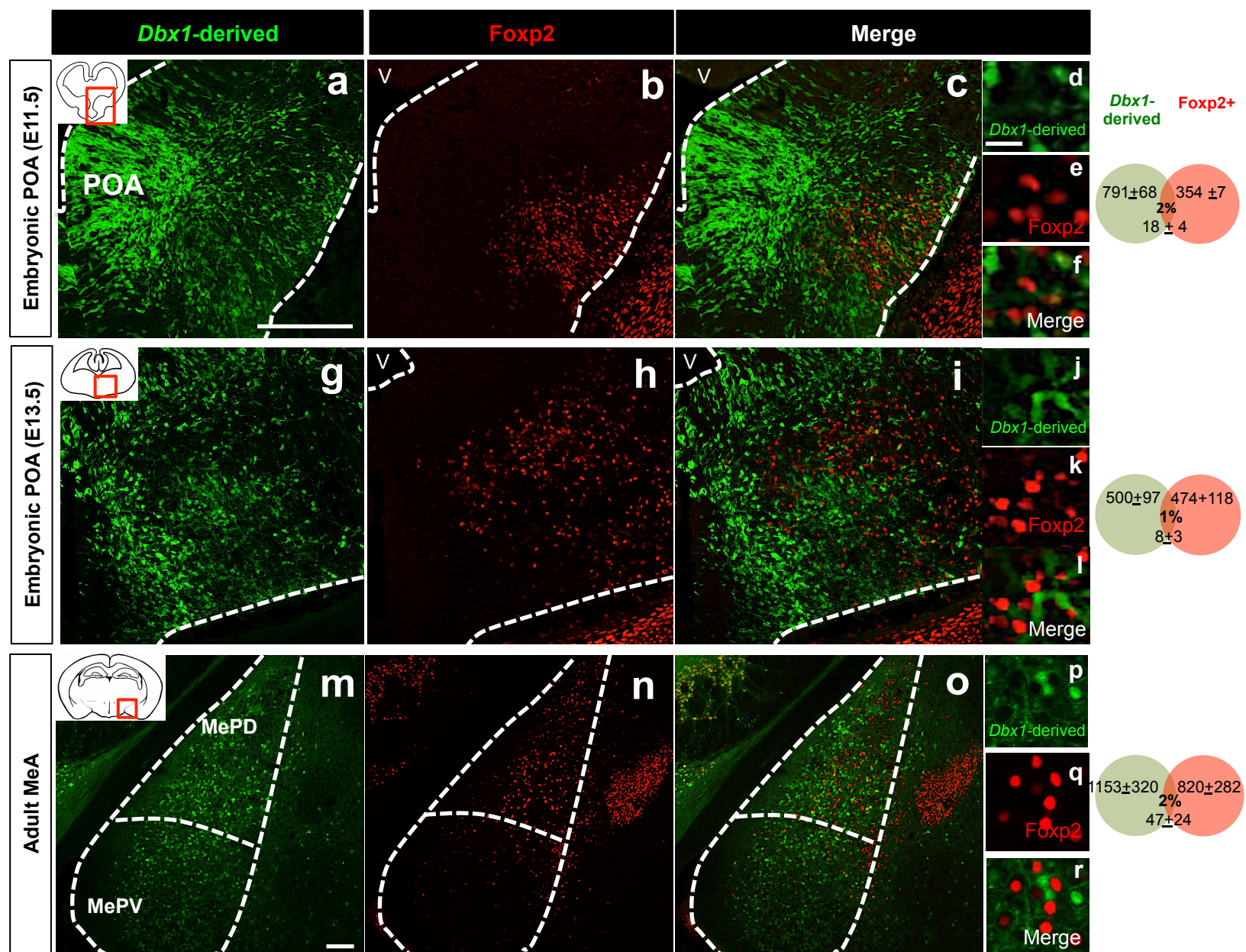
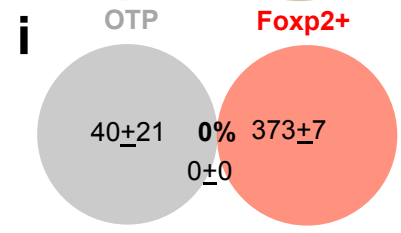
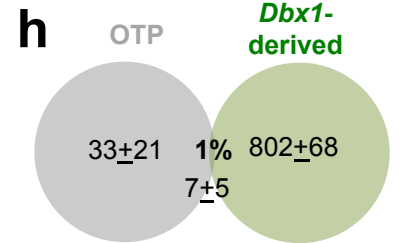
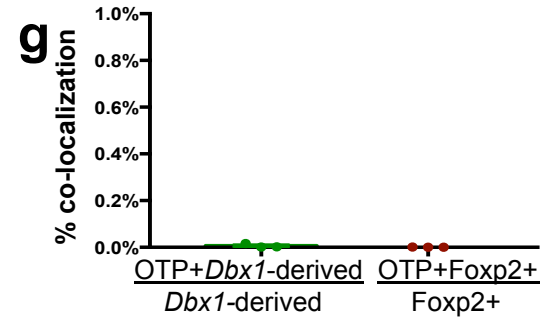
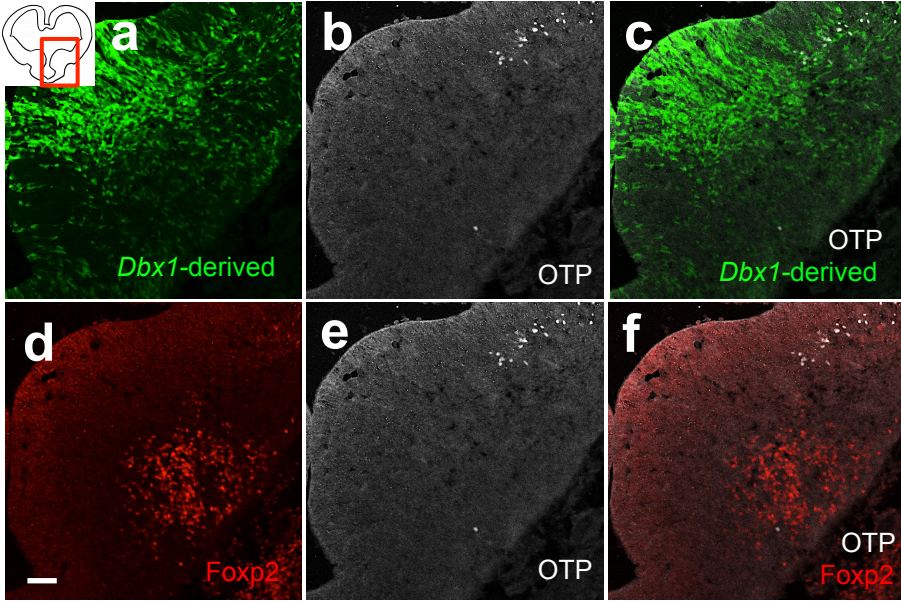


**Figure 1**

*Dbx1Cre; Rosa26YFP*

Embryonic POA (E11.5)



Postnatal

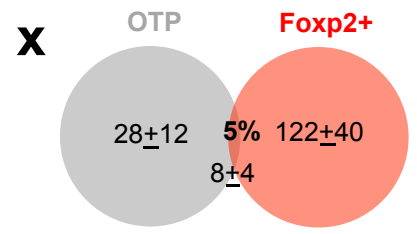
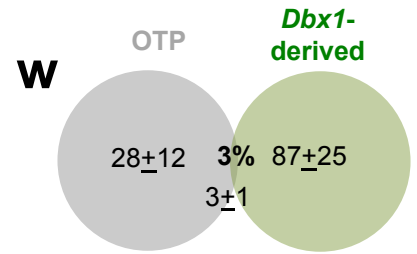
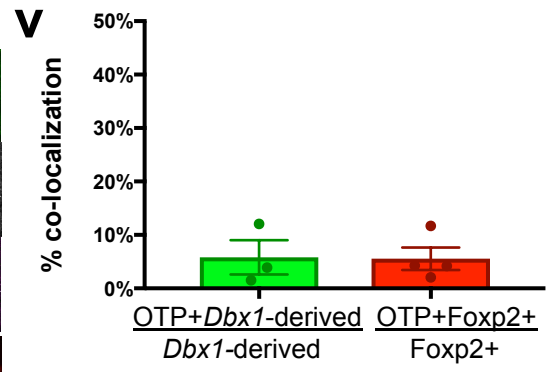
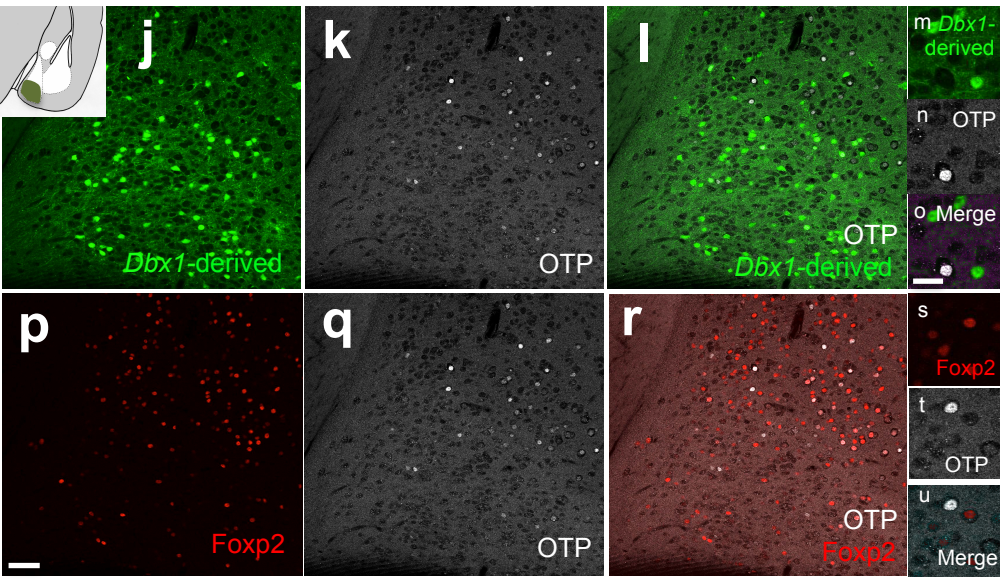


Figure 1- Figure supplement 1

Embryonic POA (E11.5)

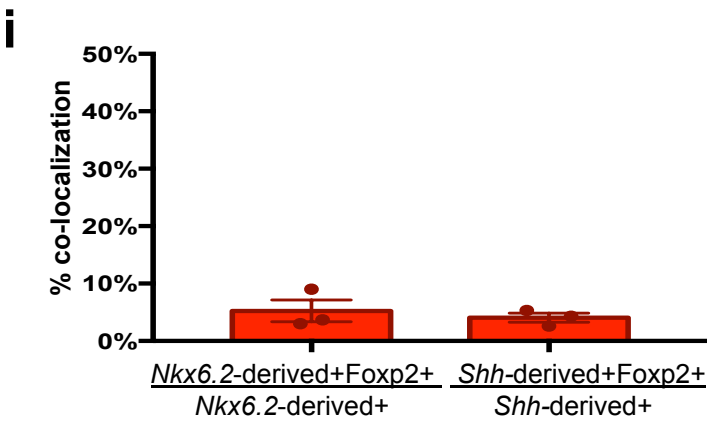
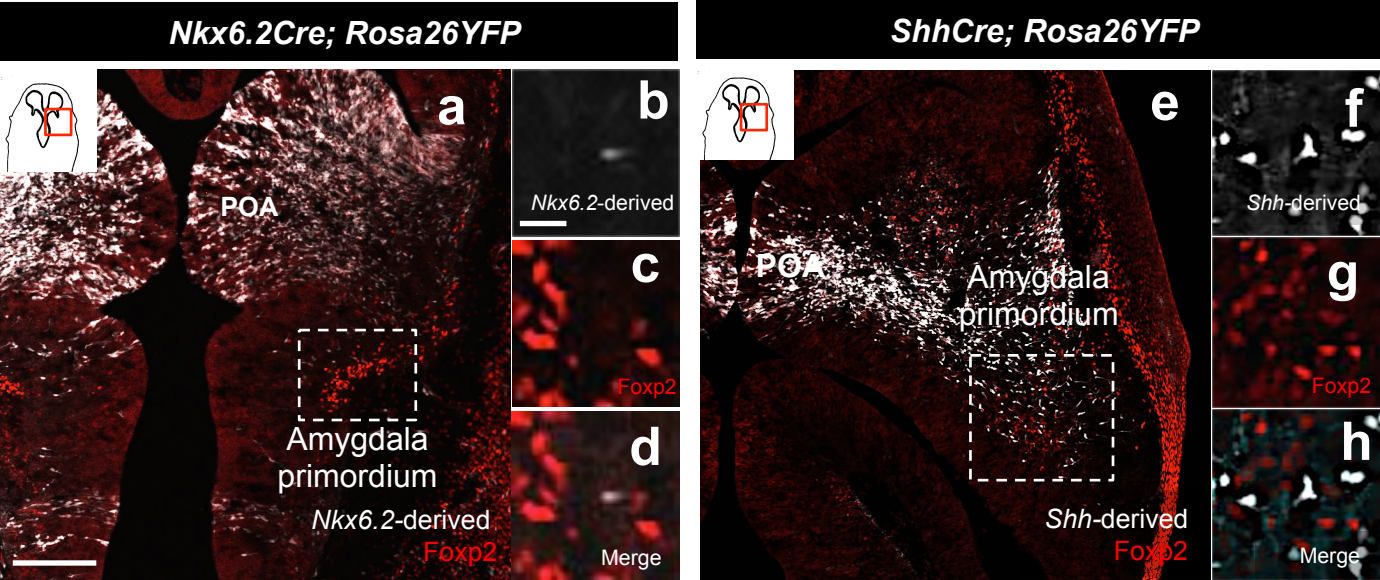
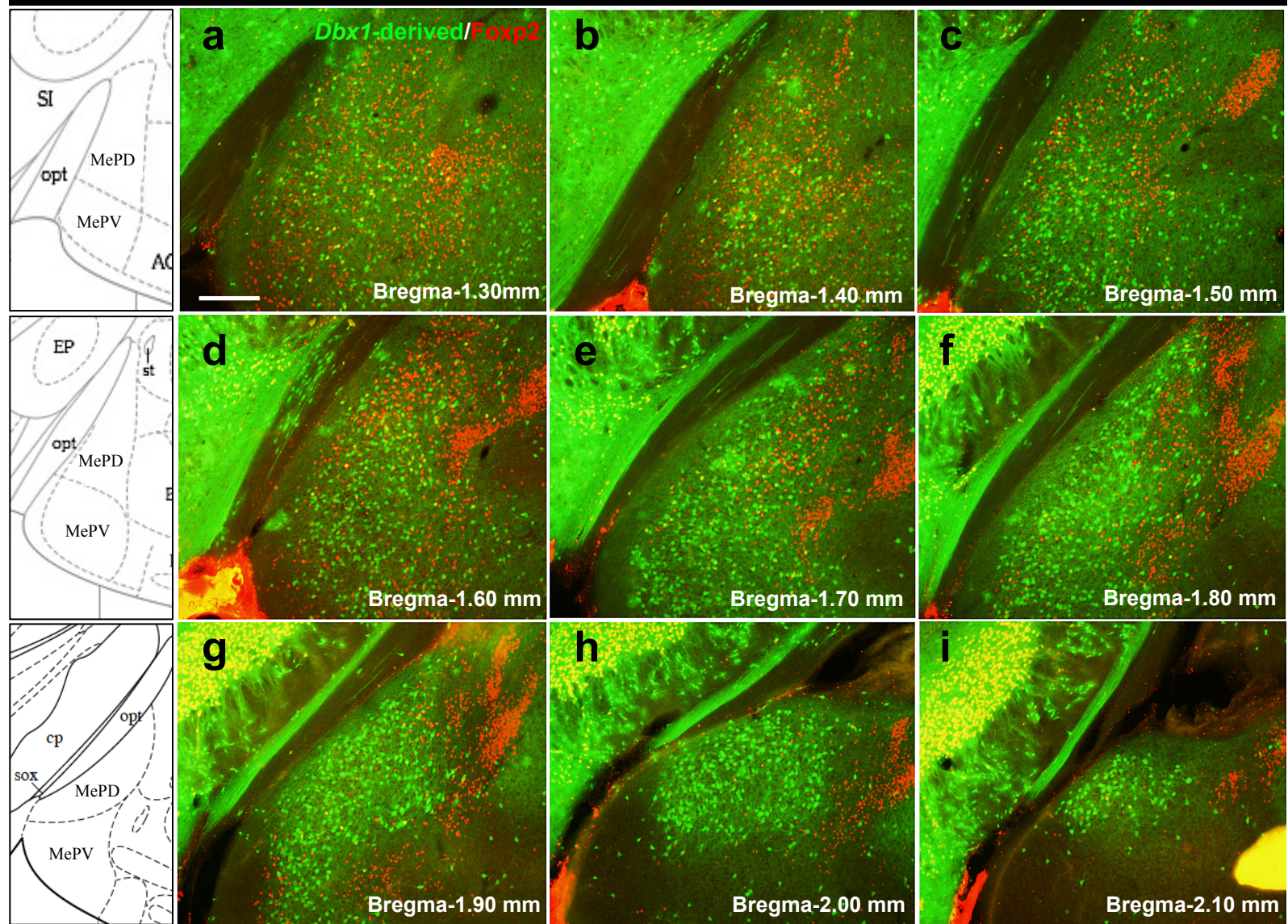


Figure 1- Figure supplement 2



*Dbx1Cre; Rosa26YFP*



**Figure 1- Figure supplement 3**

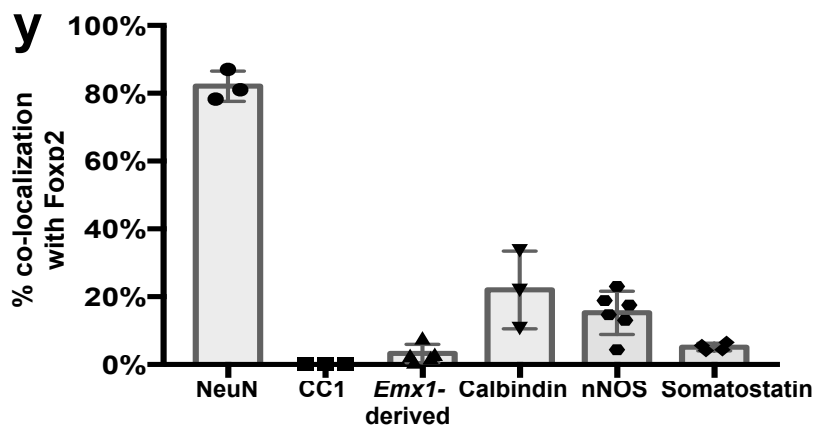
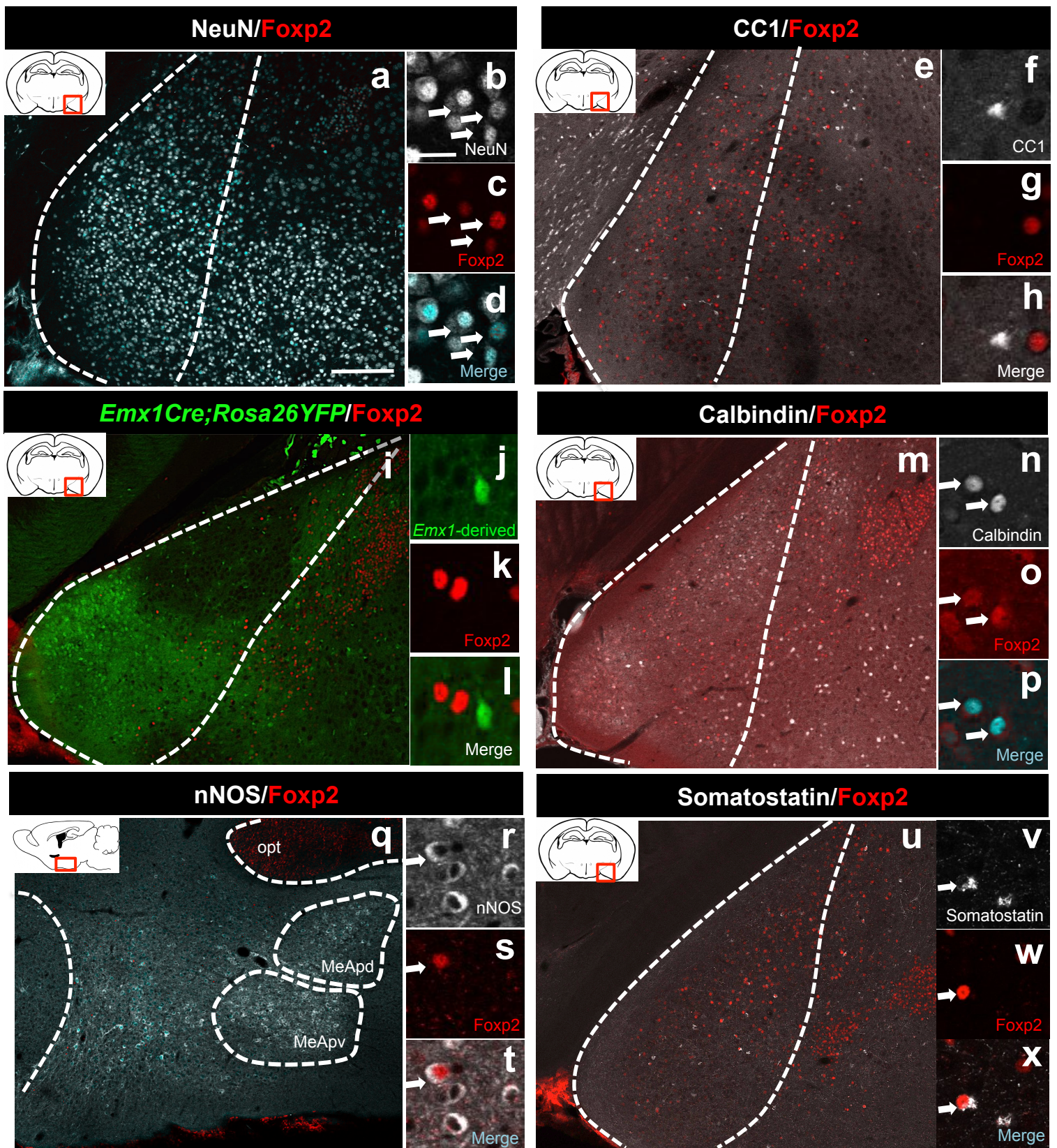


Figure 2

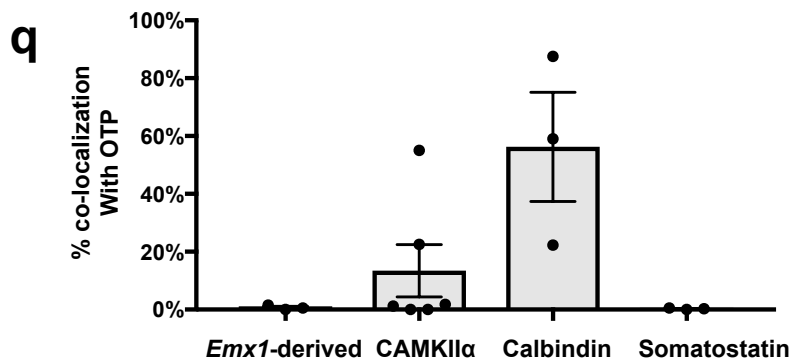
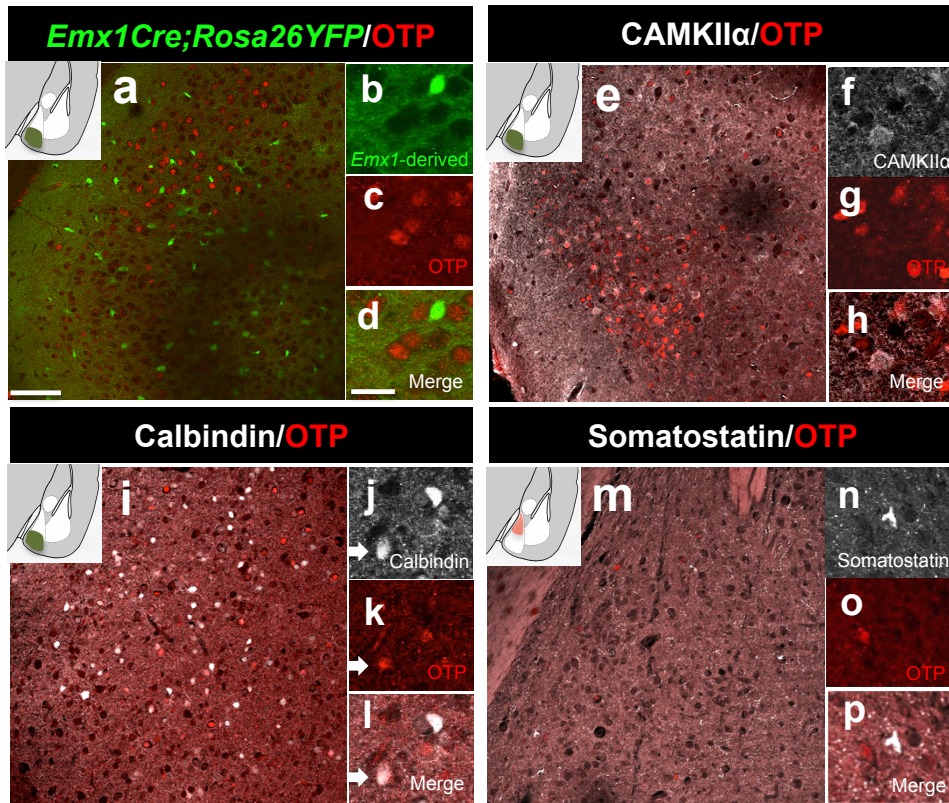
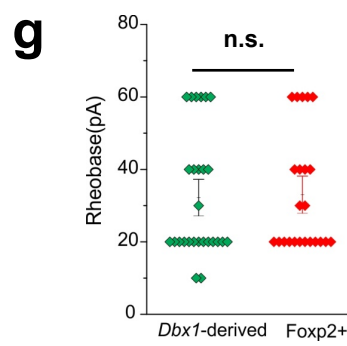
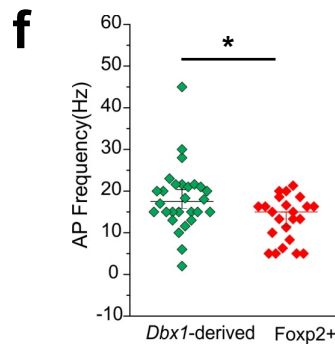
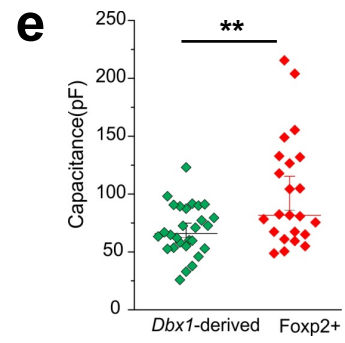
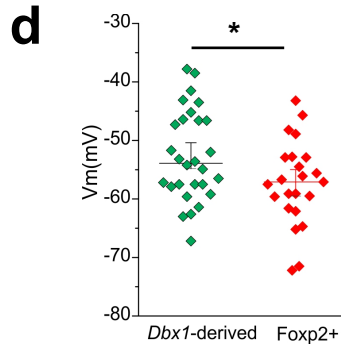
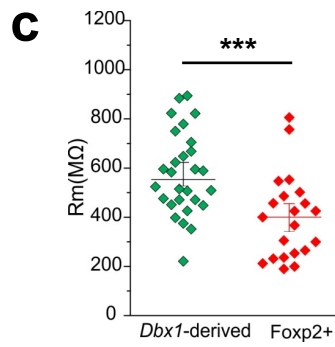
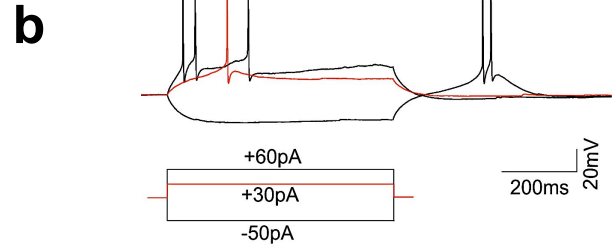
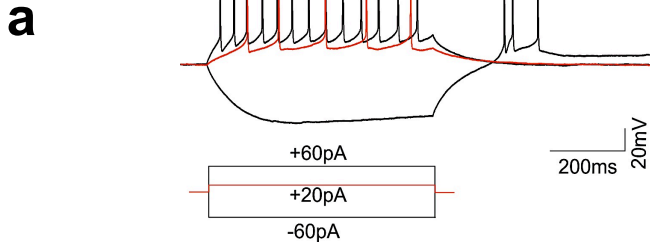


Figure 2- Figure supplement 1

# Intrinsic electrophysiological properties

**Dbx1-derived**

**Foxp2+**



# Extrinsic electrophysiological properties

**Dbx1-derived**

**Foxp2+**

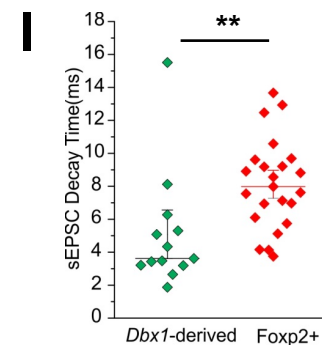
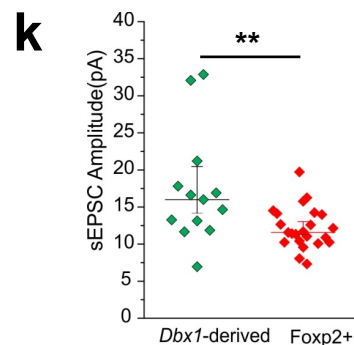
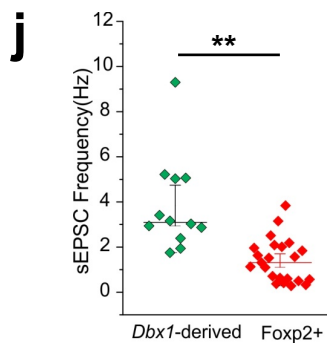
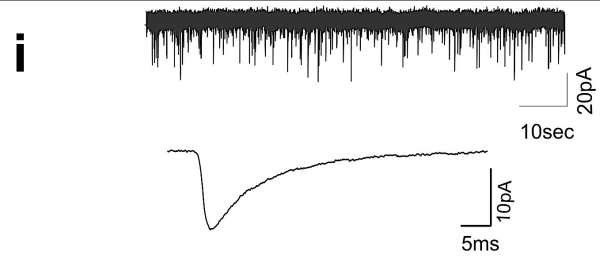
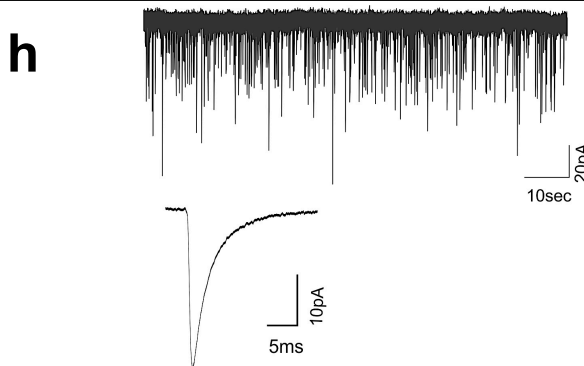


**Figure 3**

# Foxp2+ Neuronal Morphologies

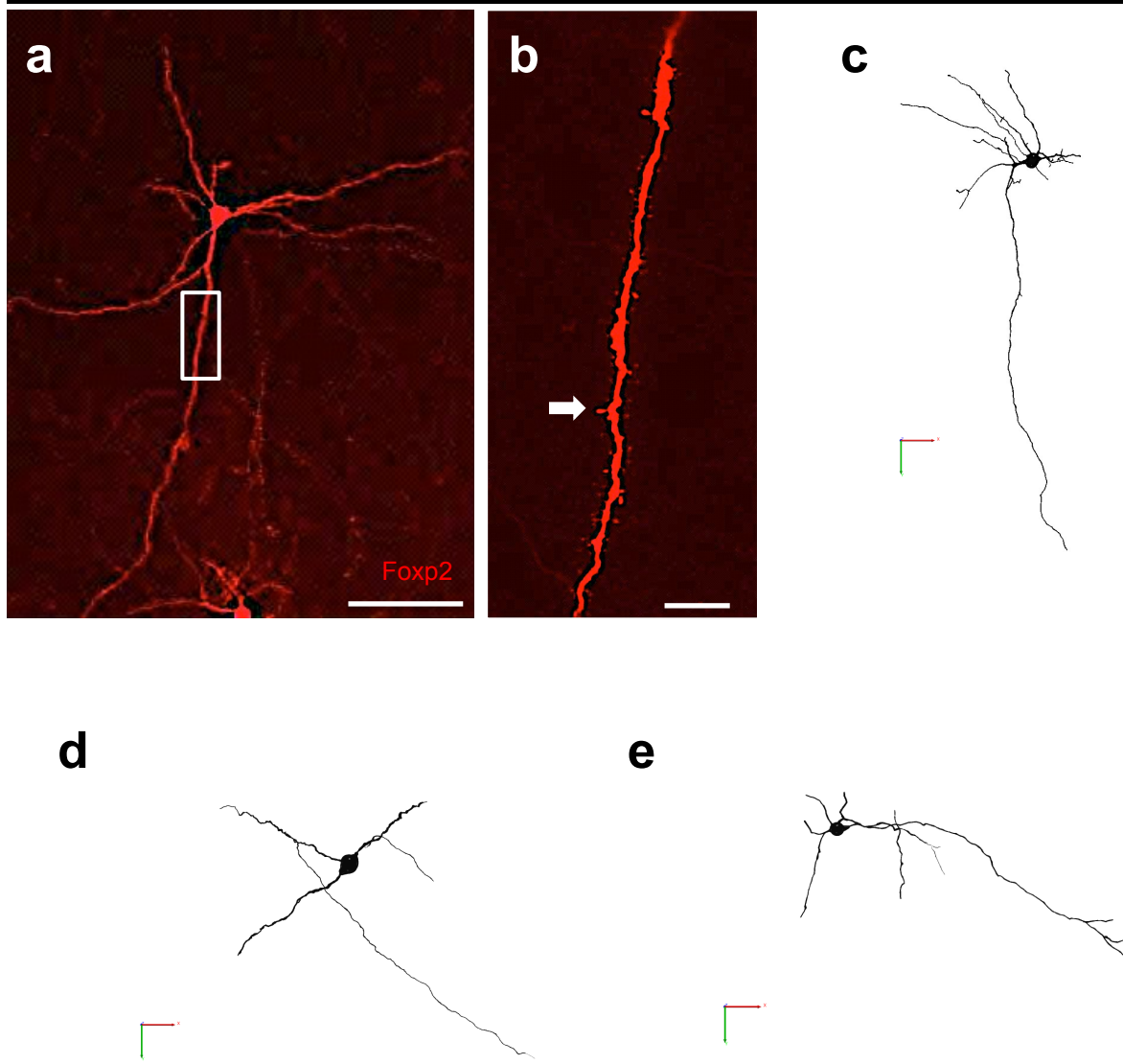
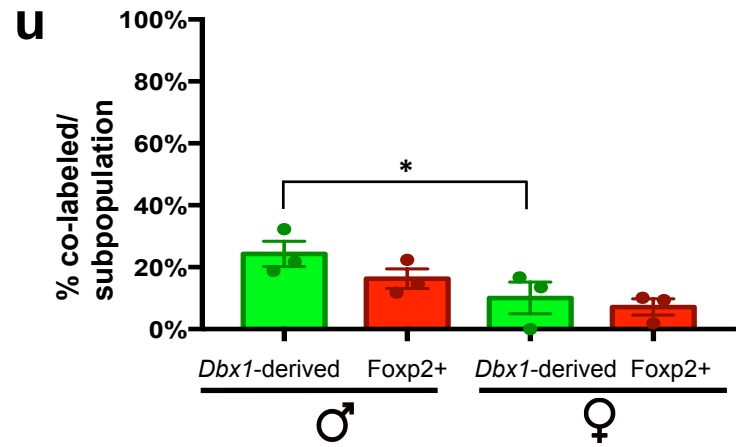
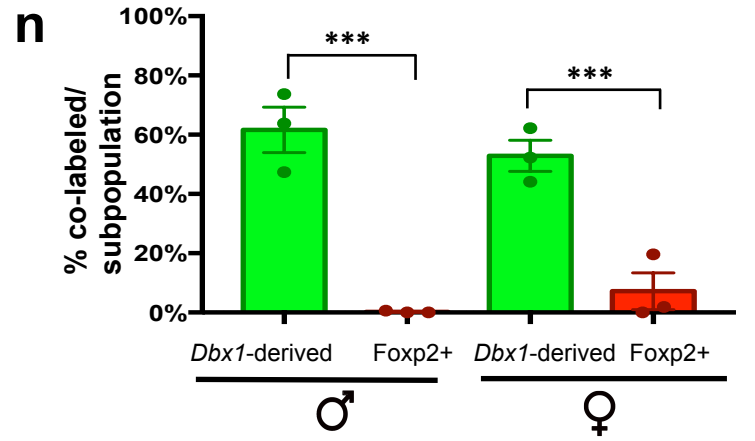
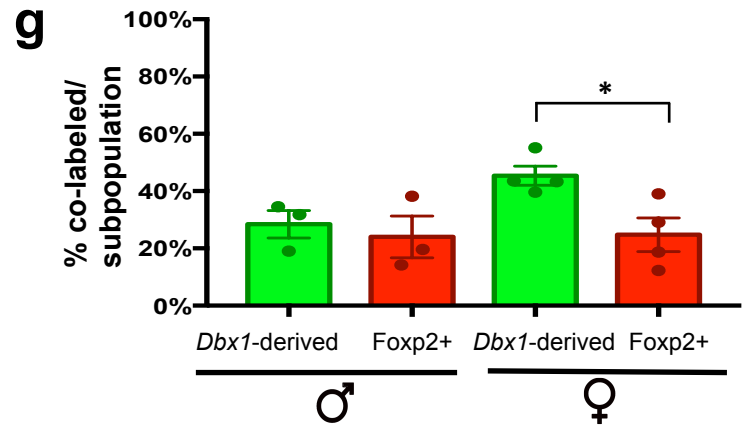
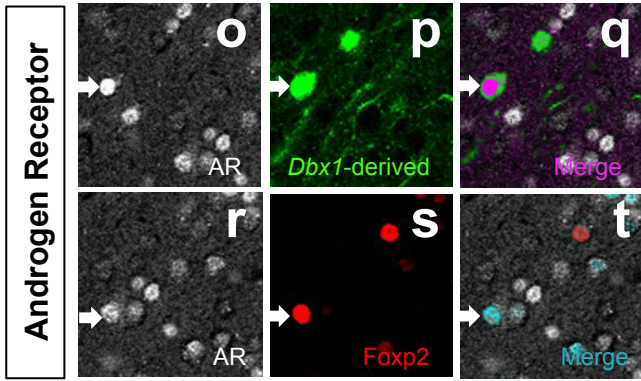
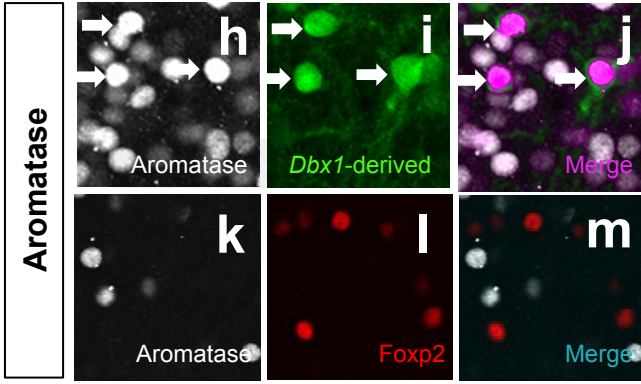
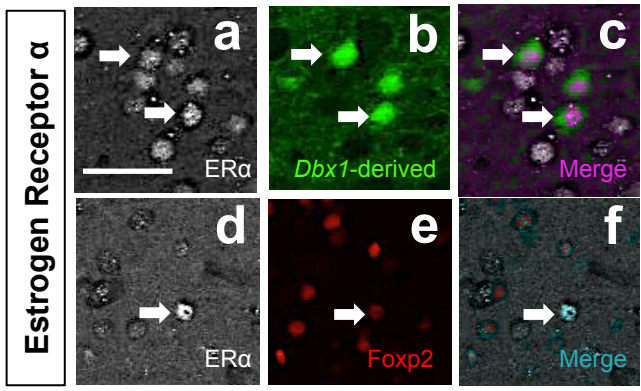
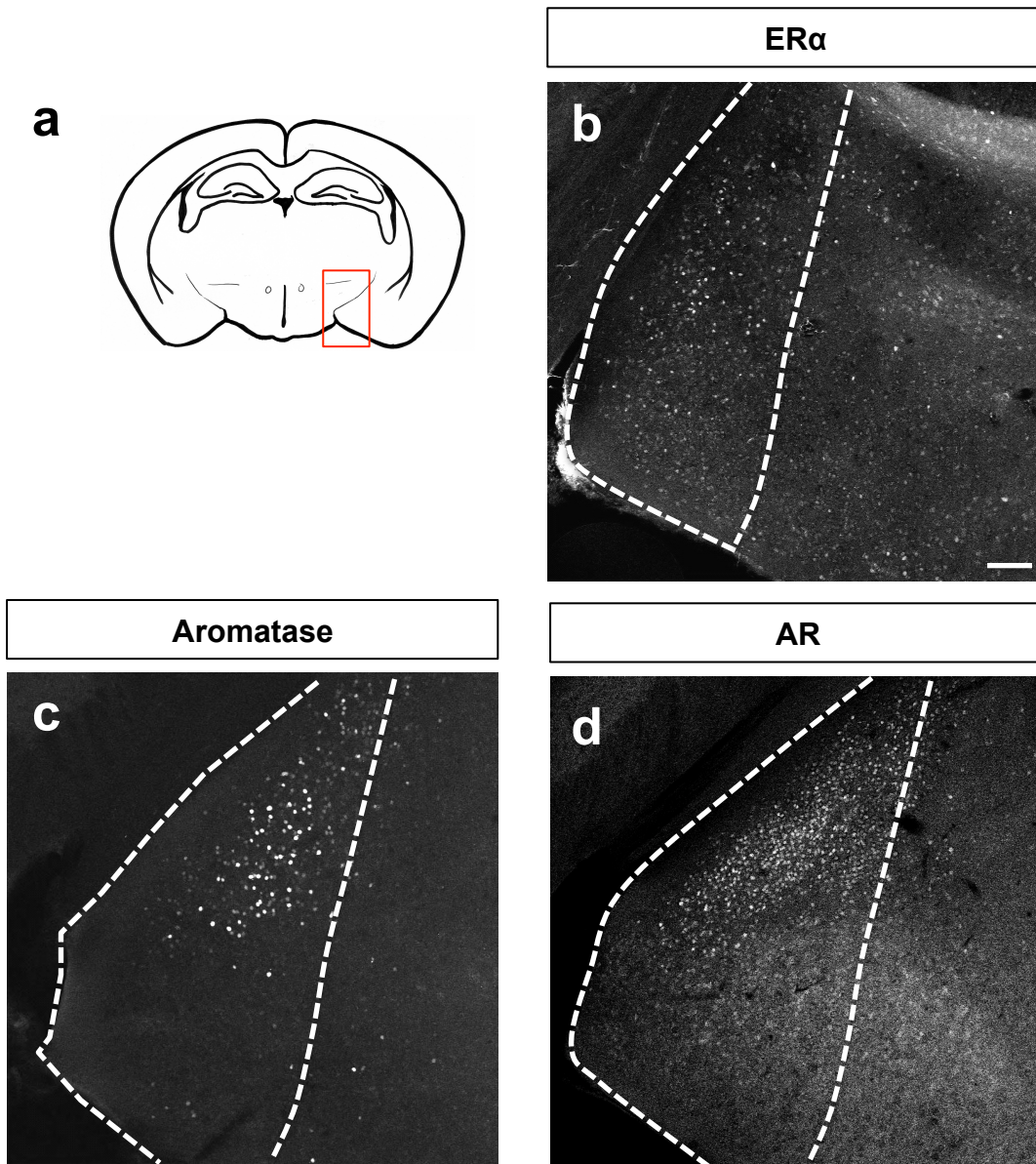


Figure 3- Figure supplement 1



**Figure 4**



**Figure 4- Figure supplement 1**

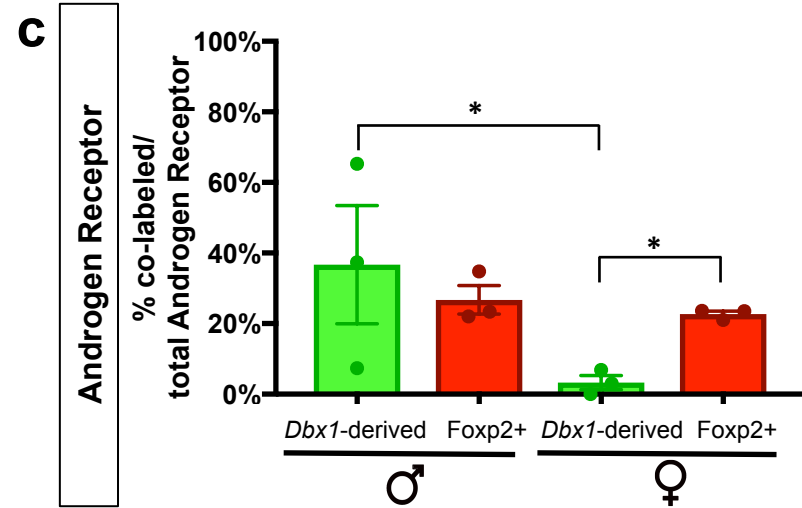
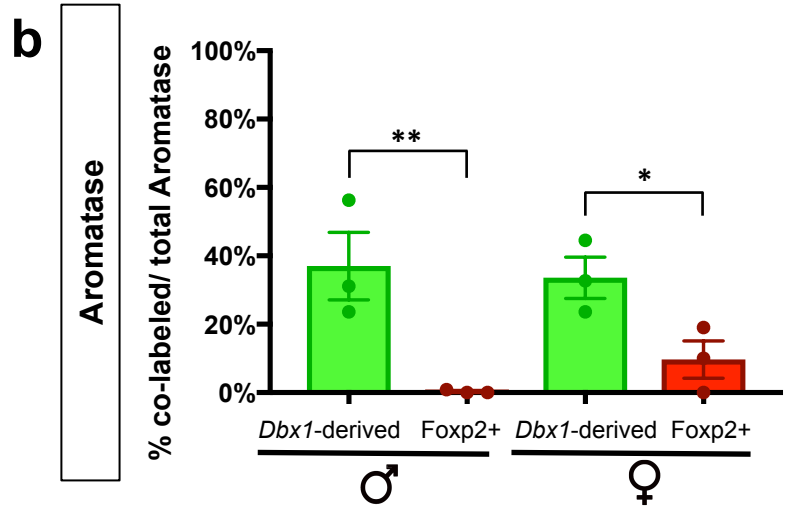
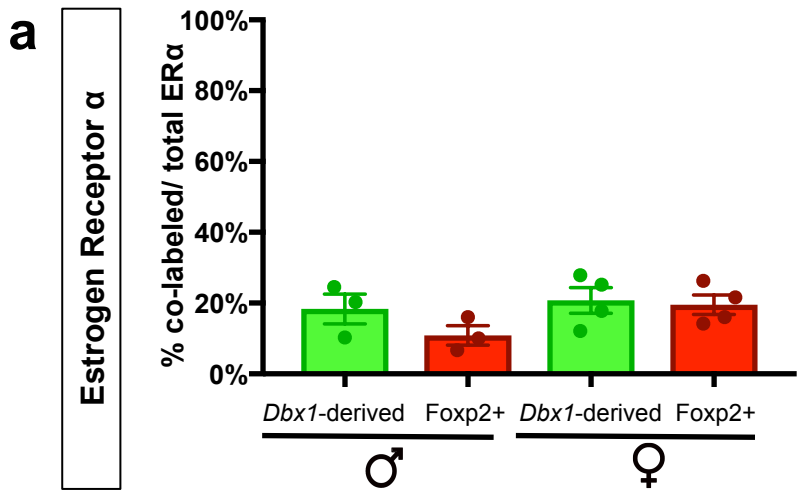
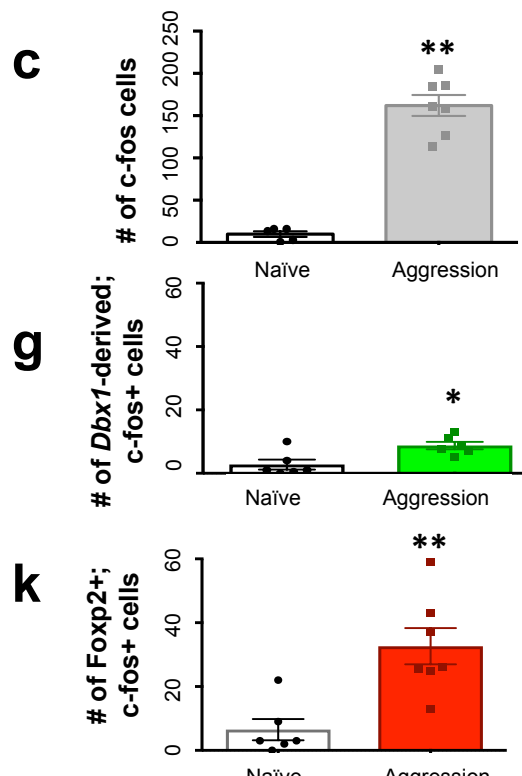
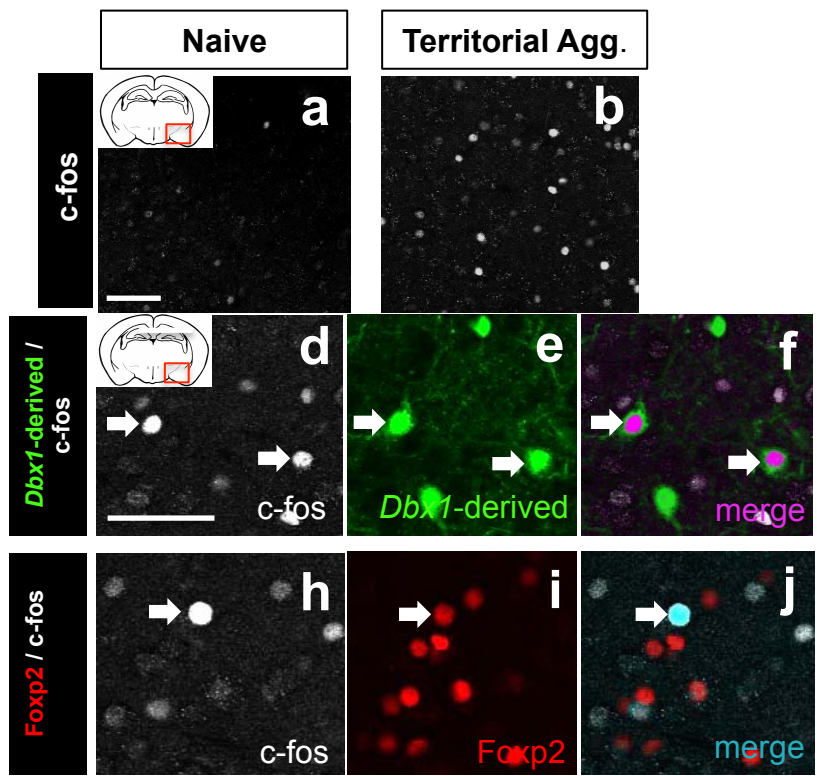


Figure 4- Figure supplement 2

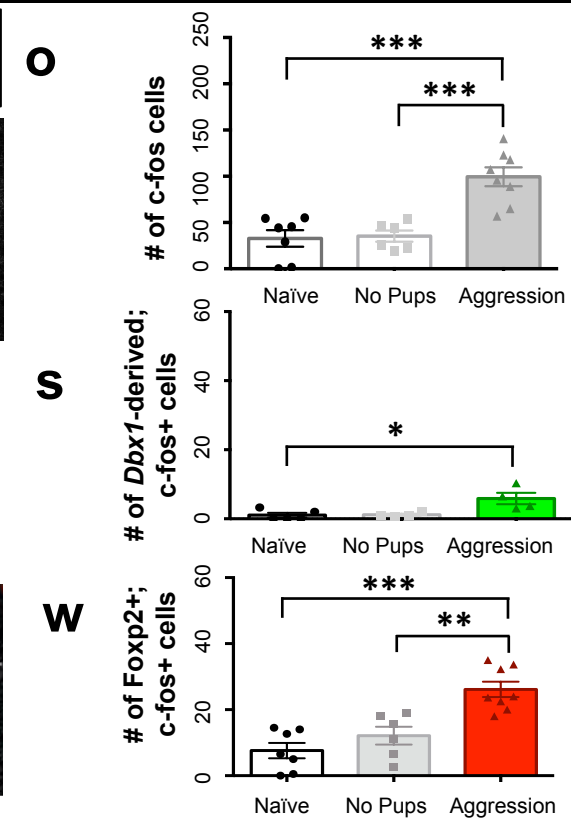
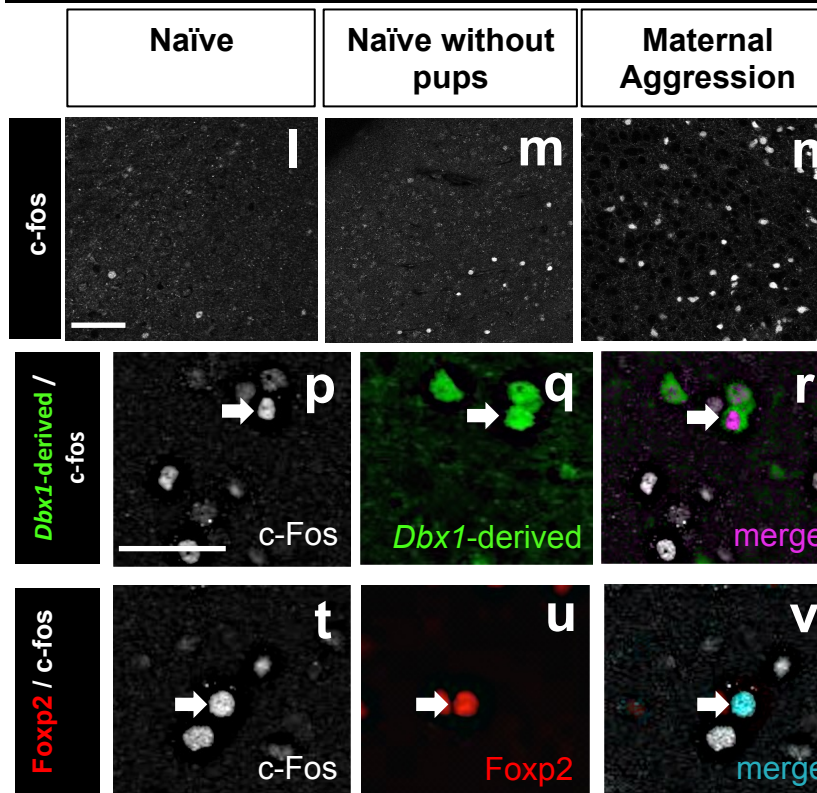


**Figure 5**

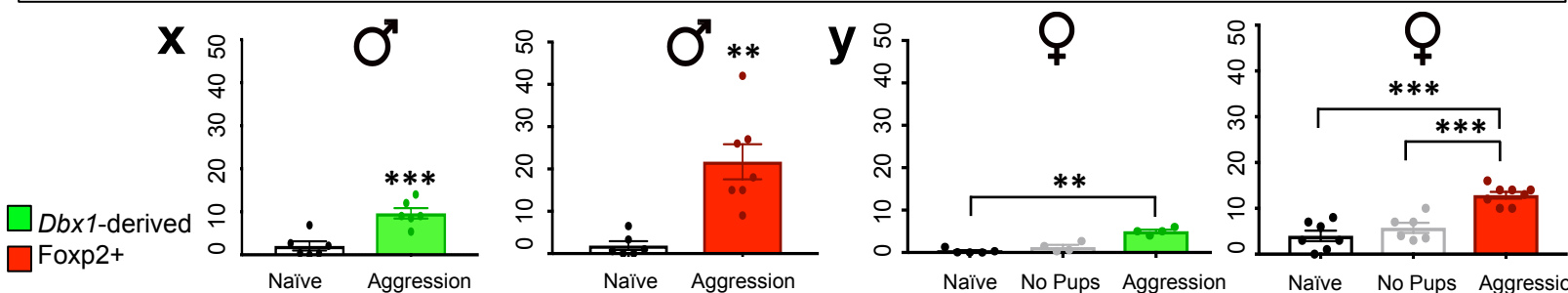
**Territorial Aggression**



**Maternal Aggression**



**% of Dbx1-derived or Foxp2 cells co-labeled with c-fos/total Dbx1-derived or Foxp2 cells**



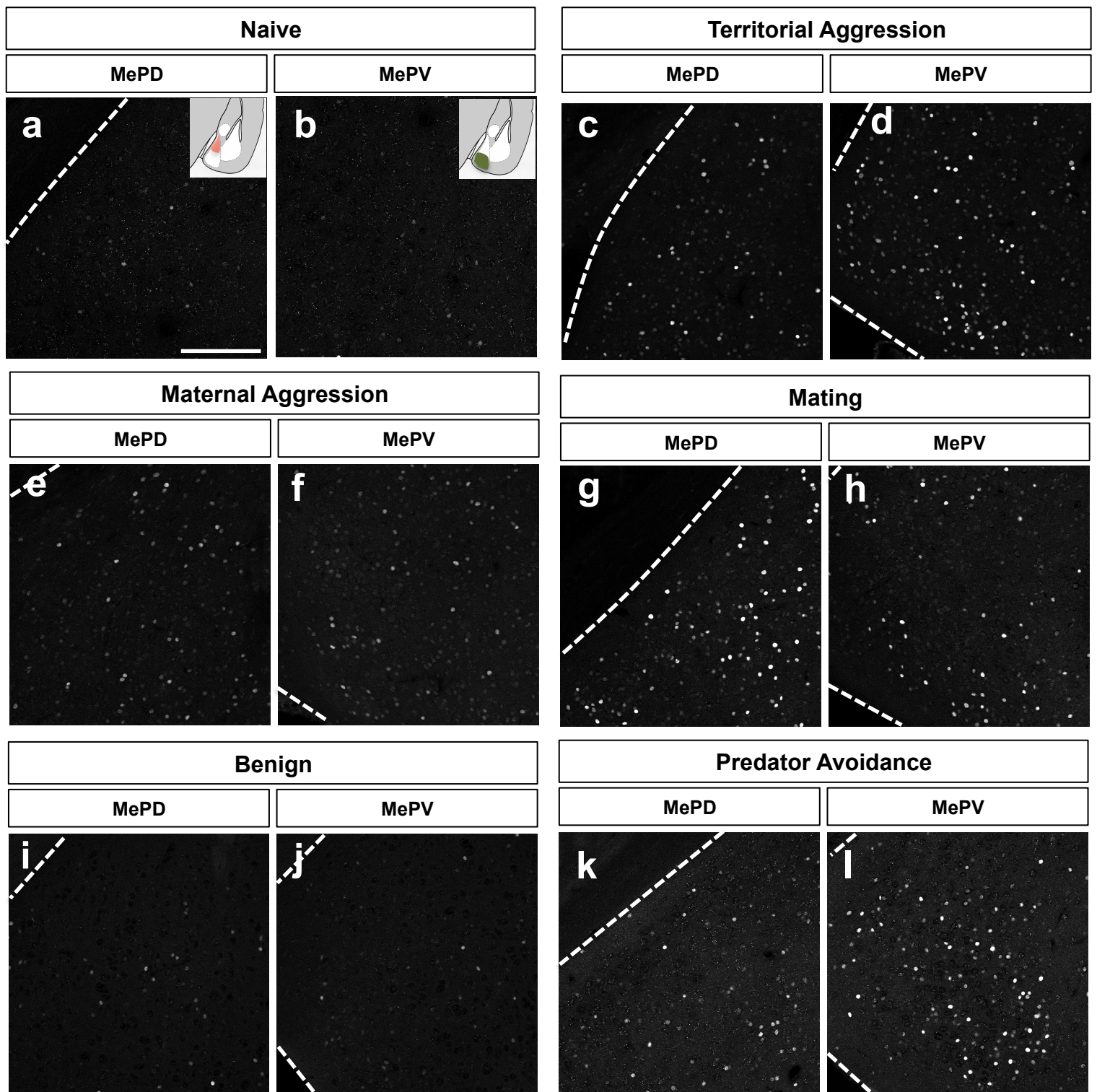
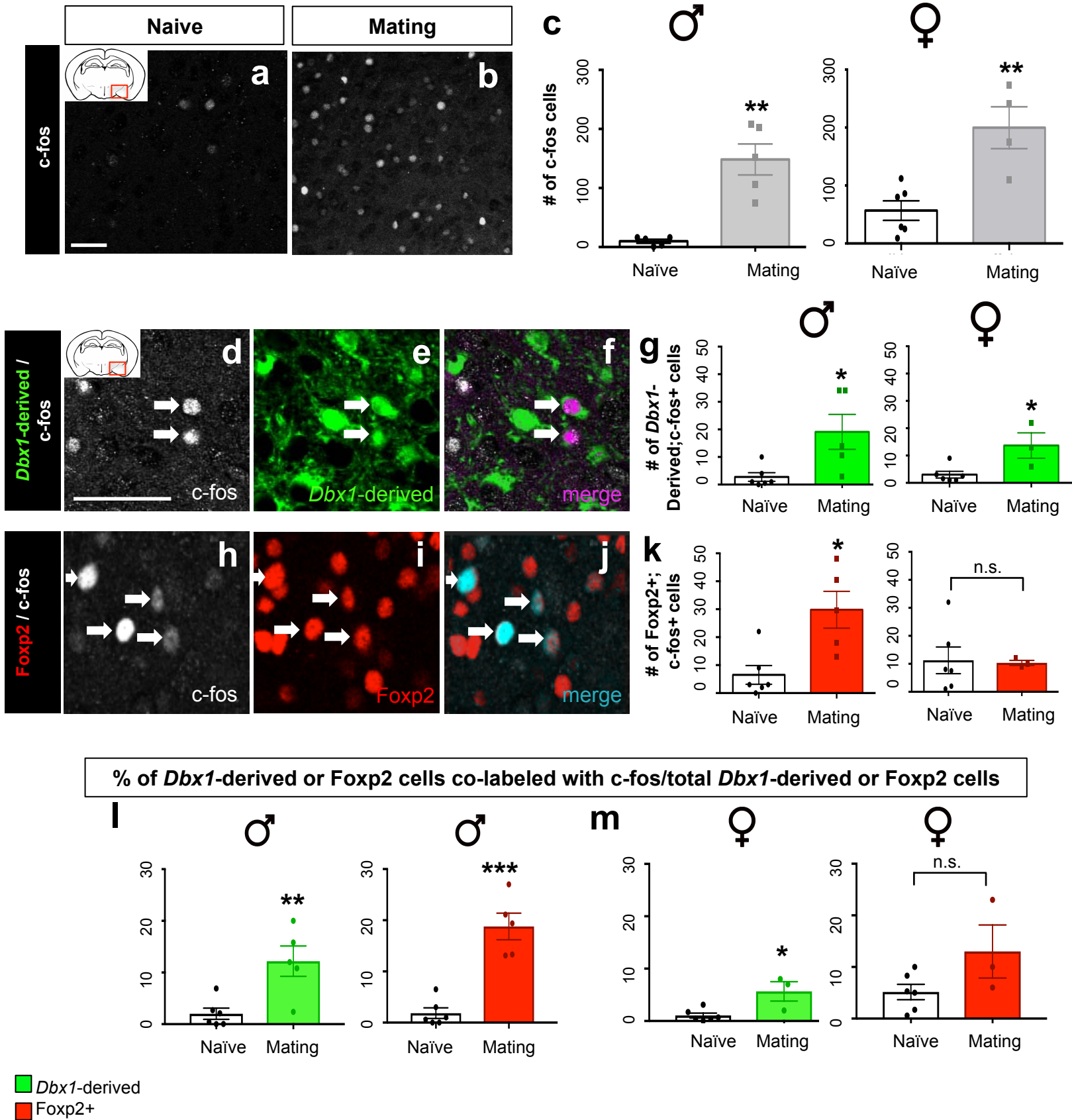
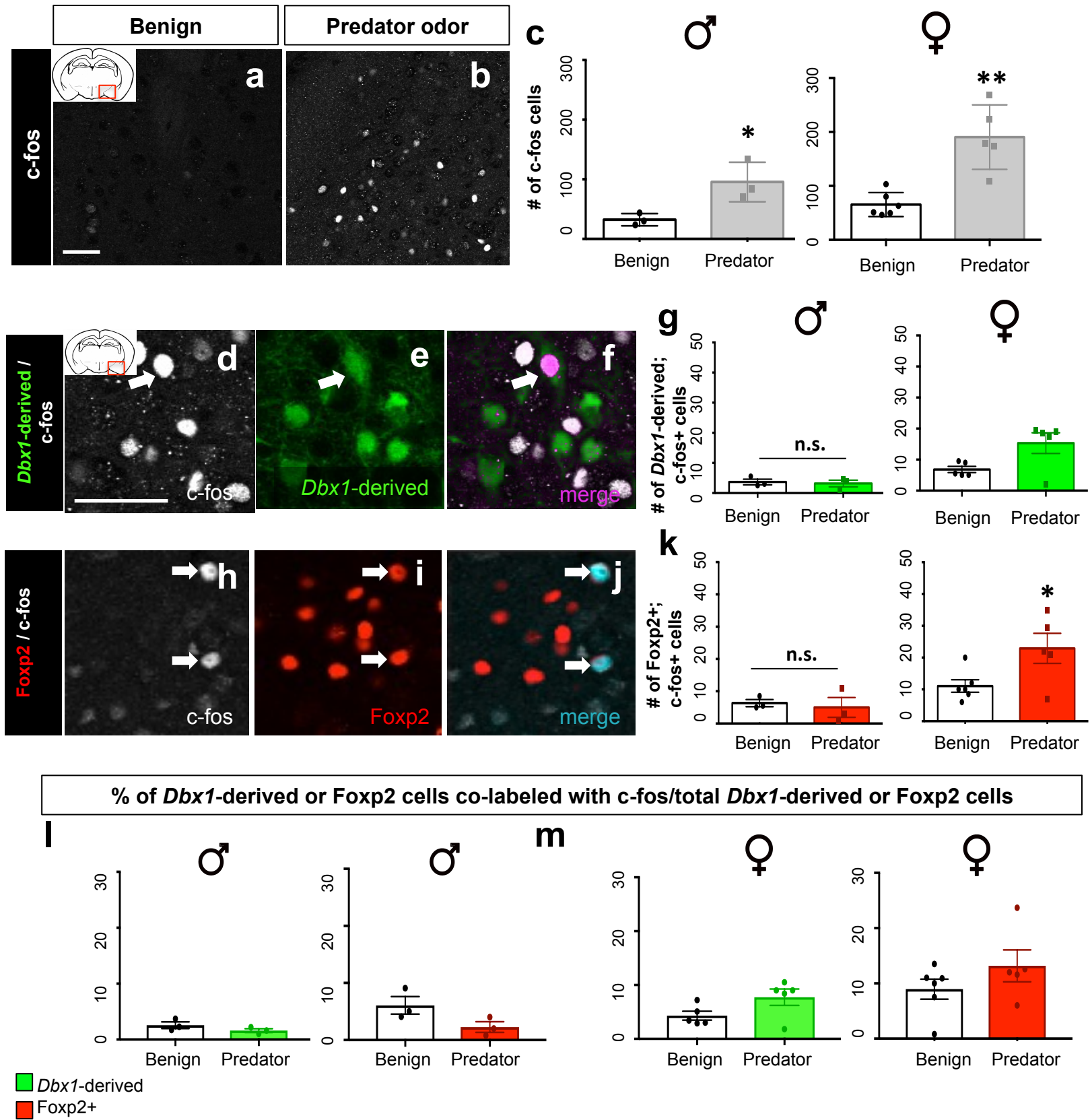


Figure 5- Figure supplement 1

# Mating



# Predator Avoidance



**Figure 7**

# Predator Avoidance

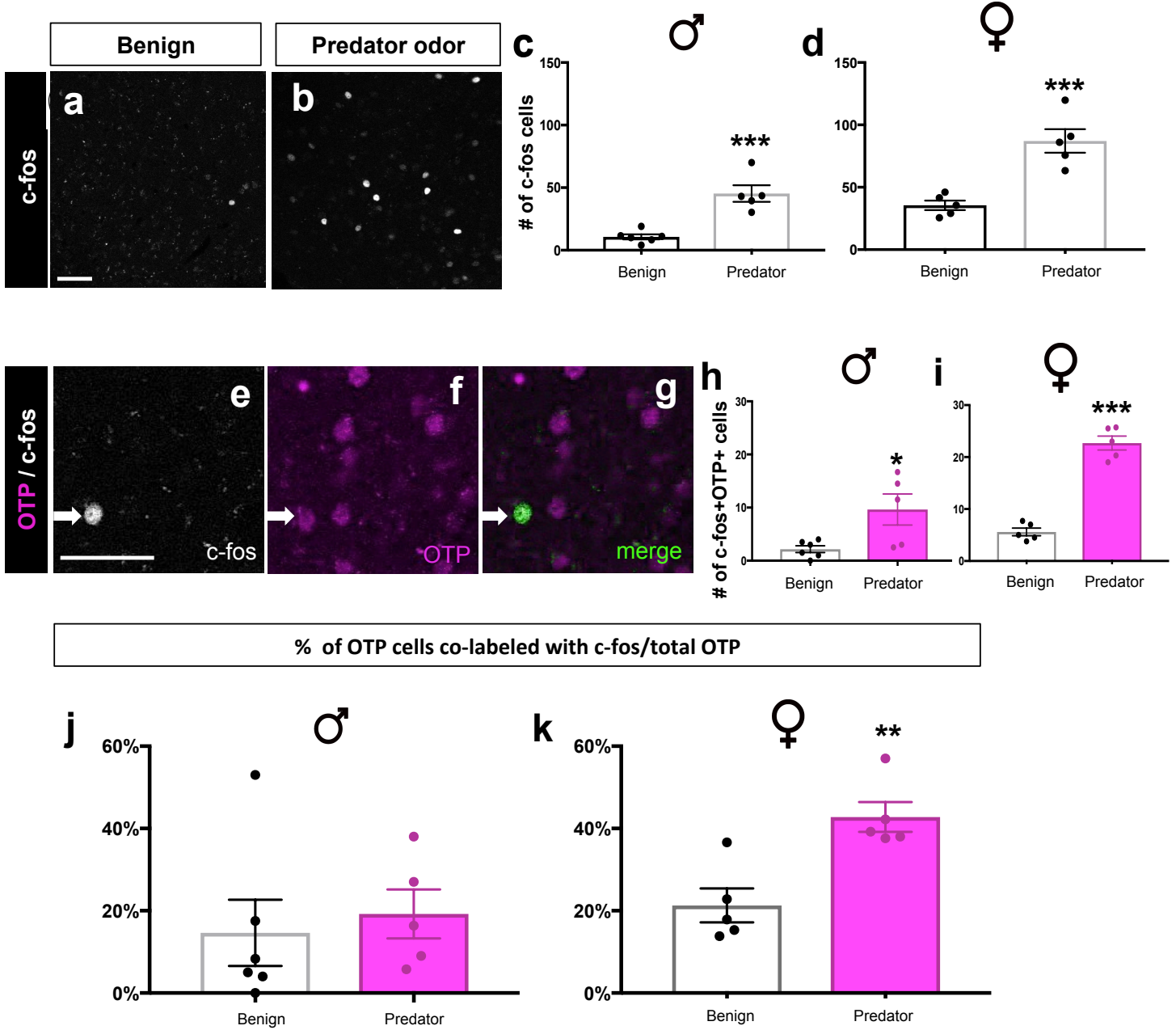
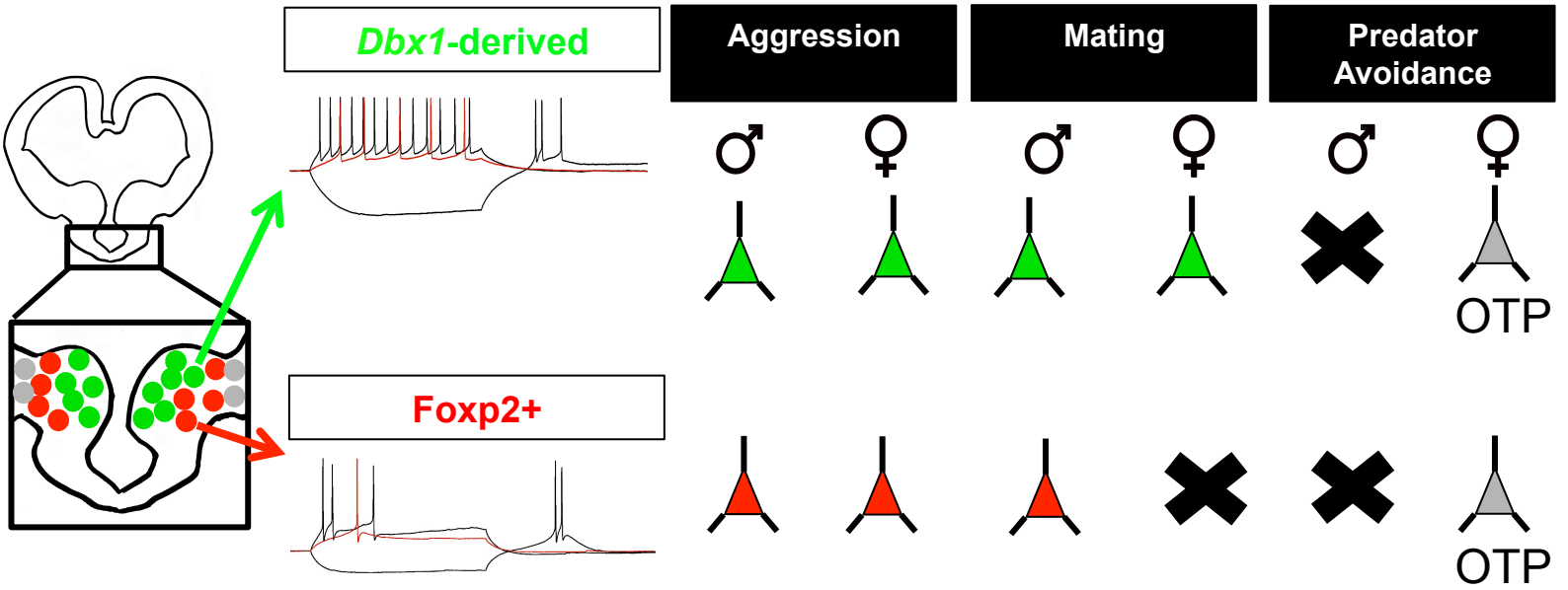


Figure 7- Figure Supplement 1



- *Dbx1*-derived
- *Foxp2*+
- *OTP*+